

---

Masters Theses

Student Theses and Dissertations

---

1962

## Neutron flux mapping of the MSM reactor

Cary Chow-Yuen Chen

Follow this and additional works at: [https://scholarsmine.mst.edu/masters\\_theses](https://scholarsmine.mst.edu/masters_theses)



Part of the [Physics Commons](#)

Department:

---

### Recommended Citation

Chen, Cary Chow-Yuen, "Neutron flux mapping of the MSM reactor" (1962). *Masters Theses*. 2908.  
[https://scholarsmine.mst.edu/masters\\_theses/2908](https://scholarsmine.mst.edu/masters_theses/2908)

This thesis is brought to you by Scholars' Mine, a service of the Missouri S&T Library and Learning Resources. This work is protected by U. S. Copyright Law. Unauthorized use including reproduction for redistribution requires the permission of the copyright holder. For more information, please contact [scholarsmine@mst.edu](mailto:scholarsmine@mst.edu).

NEUTRON FLUX MAPPING OF THE  
MSM REACTOR

BY

CARY, CHOW-YUEN, CHEN

---

A

THESIS

submitted to the faculty of the  
SCHOOL OF MINES AND METALLURGY OF THE UNIVERSITY OF MISSOURI  
in partial fulfillment of the requirements for the

Degree of

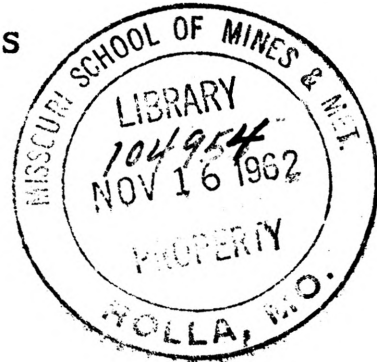
MASTER OF SCIENCE, PHYSICS

Rolla, Missouri

1962

---

Approved by



J. B. Pauls

(advisor)

Charles C. McFarland

R. A. Kent

Arnon J. Miles

## ABSTRACT

This investigation presents a mean to determine thermal neutron flux of a reactor by irradiating copper wires inside the fuel elements. The activity recorded after decay correction, is the relative thermal neutron density. Thermal neutron flux is a measure of the neutron density at thermal energy, 0.025 ev.

Gold foils irradiated at National Bureau of Standards were used as the absolute neutron flux calibration standards. The average flux of the reactor with water as the reflector ranges from  $7.24 \times 10^{10}$  neutrons/cm<sup>2</sup> - sec. to  $7.87 \times 10^{10}$  neutrons/cm<sup>2</sup> - sec. as obtained from the calculations. This set of values compares favorably with the result as measured by the manufacturers.

In this investigation the thermal neutron flux in the MSM reactor was determined by irradiating copper wires inside the fuel elements.

## ACKNOWLEDGEMENT

The author desires to express sincere gratitude to Dr. Franklin Pauls for his guidance, criticism, and assistance throughout this investigation. Much thanks are due to Professor Archie W. Culp, Jr., of the Mechanical Engineering Department, who took a special interest in this work and gave many helpful suggestions.

The author is also indebted to the reactor staff for many types of assistance. The wire counting apparatus constructed by the staff, has proved most useful and convenient.

## TABLE OF CONTENTS

	Page
ABSTRACT .....	ii
ACKNOWLEDGEMENTS .....	iii
TABLE OF CONTENTS .....	iv
LIST OF ILLUSTRATIONS .....	vi
LIST OF TABLES .....	vii
I.    INTRODUCTION .....	1
II.   REVIEW OF LITERATURE	
1.   SLOW NEUTRON ACTIVATION .....	3
2.   FAST NEUTRON ACTIVATION .....	8
III.  THEORY AND EXPERIMENTAL PROCEDURE .....	16
IV.  CONCLUSIONS .....	61
APPENDIX	
1.   SOLUTION OF THE NEUTRON ACTIVATION EQUATION.....	63
2.   RADIOACTIVITY CORRECTION FOR REACTOR START-UP	
A.   SOLUTION OF THE RADIOACTIVITY EQUATION	
FOR REACTOR START-UP .....	65
B.   PERCENTAGE CONTRIBUTION OF RADIOACTIVITY	
DUE TO THE REACTOR START-UP .....	66
3.   SAMPLE COMPUTATIONS	
A.   STANDARD FOIL COMPUTATION .....	68
B.   ABSOLUTE FLUX CALCULATION OF CORE	
POSITION F-6 AT 18 INCHES .....	68
C.   AVERAGE ABSOLUTE FLUX CALCULATION	
OF THE CORE .....	69

BIBLIOGRAPHY .....	Page 70
VITA .....	72

## LIST OF ILLUSTRATIONS

Figures		Page
1a.	Core Arrangement .....	16
1b.	Source, S, and Fuel Positions .....	17
2a.	Wire Positions for 19W .....	18
2b.	Wire Positions for 19T .....	18
3.	Wire Counting Geometry .....	20
4.	Foil Counting Geometry .....	21
5.	Foil and Wire Holders .....	22
6.	Flux Distribution of the Core for 19W .....	24
6a.	Flux Distribution of Fuel in Row F for 19W ....	25
6b.	Flux Distribution of Fuel in Row E for 19W ....	26
6c.	Flux Distribution of Fuel in Row D for 19W ....	27
6d.	Flux Distribution of Fuel in Row C for 19W ....	28
7.	Flux Distribution of the Core for 19T .....	43
7a.	Flux Distribution of the Fuel in Row F for 19T. ....	44
7b.	Flux Distribution of the Fuel in Row E for 19T. ....	45
7c.	Flux Distribution of the Fuel in Row D for 19T. ....	46
7d.	Flux Distribution of the Fuel in Row C for 19T. ....	47

## LIST OF TABLES

Table		Page
I.	Wire Activation for 19W .....	29
II.	Gold Foil Activation for 19W	
	A. Bare Gold Foils .....	40
	B. Cadmium Covered Gold Foils .....	41
III.	National Bureau of Standards Gold Foils ....	42
IV.	Wire Activation for 19T .....	48
V.	Gold Foil Activation for 19T	
	A. Bare Gold Foils .....	59
	B. Cadmium Covered Gold Foils .....	60



## I. INTRODUCTION

At the present, flux calculation for a given reactor remains a cumbersome and tedious process. At best the theoretical calculation is good as a first order approximation due to the assumptions required to make the problem practicable for solution by a computer. Thus the most accurate method of flux mapping relies on the various experimental techniques in which detectors or probes of some sort are extensively used.

A knowledge of the flux profile, although not essential in the operation of a reactor, is nonetheless important and has many uses. By the information gained from a mock-up reactor, designers can use the neutron flux profile to determine the power distribution, the locations for the control rods, thermal columns and other components which affect the neutron population. In a research reactor which is used as neutron source for radiation experiments, a knowledge of the neutron flux is most useful.

It is the purpose of the following investigation to make known the flux profiles for a few simple core arrangements. It is hoped that refinement of the present method will be made in the future. A system for automatic scan counting of the wire using a recorder will reduce the handling time and provide a continuous flux profile with minimum data processing required.

The selection of the copper wire as the detector in the activation experiments is based on its properties and handling safety. Copper-64 has an activation cross section 3.9 barns as compared to 96 barns for gold and 145 barns for indium, and is potentially safer for handling. Copper 65 has a half life of 4.3 minutes and will contribute insignificant radiation hazard after a decay time of several hours. It is estimated that a 14 gauge copper wire of 30 inches in length will give a radiation dosage of about

4 mr/hr at two feet distance when irradiated 20 minutes in a reactor of 10 kilowatt and after a waiting time of 4 half lifes. With the protection of lead shield, personnel can be safely exposed to the radioactive wire and stay within the maxium permissible exposure dosage of 100 mr per week. The commercially obtainable copper is better than 99.9% in purity and has small variation in diameter. If desired, the copper wire can be drawn into smaller diameter wire of uniform dimension with excellent surface smoothness.

## II. REVIEW OF LITERATURE

### 1. Slow Neutron Activation

Neutron flux measurements have been made successfully by radioactivation on many materials. The most commonly used materials are gold (1) and indium (2) foils.

In all such activation measurements, the procedure consists of exposing a foil of the material being used as a detector to the neutron flux for a known amount of time. Flux depression (3) due to the presence of the foil is small in most instances since the foil is of negligible thickness. The sample is removed and its radioactivity measured by observing the number of counts in a given time interval. If this procedure is repeated with a foil wrapped with cadmium (4), the foil will then be activated only by neutrons with energies above the cadmium cutoff, about 0.4 ev. The difference between the number of counts obtained from the two exposures can be related to the thermal flux if the detector's cross section is inversely proportional to the neutron velocity.

The number of capturing events or the activation response is proportional to  $nv\sigma$ , where  $n$  is the neutron density,  $v$  is the velocity of the neutrons, and  $\sigma$  is the microscopic cross section of the detector, thus

$$\text{Thermal response} \propto (nv)_{\text{th}} \sigma_{\text{th}} \quad (2-1)$$

and

$$\text{Resonance response} \propto \int_{0.4 \text{ ev}}^{\infty} \sigma_a(E) \phi(E) dE \quad (2-2)$$

$\phi(E)$  is the resonance neutron flux per unit energy, and  $\sigma_a(E)$  is the microscopic absorption cross section at energy  $E$ . For neutron flux in the resonance region which varies as  $1/E$ , equation (2-2) can be represented as

$$\text{Resonance response} \propto \int_{0.4 \text{ ev}}^{\infty} \sigma_a \phi_{\text{res}} dE/E \quad (2-3)$$

where  $\phi_{\text{res}}$  is a constant.

The cadmium ratio,  $R_{\text{cd}}$ , is defined as the ratio of the sum of thermal and resonance response to the resonance response, it is evident that

$$R_{\text{cd}} - 1 = \frac{\text{thermal response}}{\text{resonance response}} = \frac{(nv)_{\text{th}} \sigma_{\text{th}}}{\phi_{\text{res}} \int_{0.4 \text{ ev}}^{\infty} \sigma_a (E) dE/E}$$

The actual cadmium ratio observed is a function of the sensitivity of the detector to resonance and thermal neutrons and does not lead to the true flux ratio unless this sensitivity is known. If the value for the thermal cross section and the resonance integral are known, then the ratio of the thermal and resonance fluxes can be obtained. As stated before, the thermal response can be found by the difference between the uncovered exposure which measures the total response, and the cadmium covered exposure which measures the resonance response. The absolute resonance flux can be obtained if some standard is available for converting thermal response to absolute thermal flux.

Some materials have one sharp resonance which predominates, and effectively all the resonance neutrons absorbed by the detector are neutrons which have energies grouped about the resonance peak. In such a case,

$$\int_{0.4 \text{ ev}}^{\infty} \sigma_a (E) \phi (E) dE = \phi (E_r) \int_{0.4 \text{ ev}}^{\infty} \sigma_a (E) dE \quad (2-5)$$

where  $\phi (E_r)$  is the resonance flux per unit energy corresponding to the resonance peak, since the integral is largely determined by the energy interval in the neighborhood of the resonance peak. A flux spectrum over a considerable range of energies can be obtained by activating materials which have prominent resonance absorption at various energies.

Employing the activation principle, Battelle Memorial Institute (5) investigated a flux profile by the activation of magnesium-indium wire. A cadmium-alloy tubing was used to simulate the cadmium cover used in the foil-activation technique. A continuous counting device with gears and timer was developed. The method used is practicable under conditions of relatively high flux level and is more expeditious compared to the foil activation technique.

Another method of neutron detection is by means of a  $\text{BF}_3$  counter. The reaction,  $\text{B}^{10} (n, \alpha) \text{Li}^7$ , enables the detection of neutrons by the ionization caused by alpha particles. The rate of neutron capture events in a volume,  $V$ , of  $\text{BF}_3$  gas possessing  $N$  atoms of  $\text{B}^{10}$  per  $\text{cm}^3$  is

$$R = NV \int_0^{\infty} n(v) v \sigma(v) dv \quad (2-6)$$

where  $n(v)$  is the neutron density per unit velocity interval at velocity  $v$ , and  $\sigma(v)$  is the  $\text{B}^{10}$  capture cross section at velocity  $v$ .

When detecting neutrons in the thermal region,  $\sigma(v)$  is nearly proportional to  $1/v$ , and it may be written as

$$\sigma(v) = \frac{\sigma_0 v_0}{v} \quad (2-7)$$

where  $\sigma_0$  is the thermal capture cross section for  $\text{B}^{10}$  and  $v_0$  is the most probable neutron velocity. Then the rate of neutron capture is

$$R = NV \sigma_0 v_0 \int_0^{v_0} n(v) dv = NV \sigma_0 v_0 \rho \quad (2-8)$$

where  $\rho$  is the density of slow neutrons.

If the velocity spectrum,  $n(v)$  is well known about an average velocity  $\bar{v}$ , then the flux density is given by

$$\rho \bar{v} = \frac{R \bar{v}}{NV \sigma_0 v_0} \quad (2-9)$$

The measurement of R, the rate of  $B^{10}$  capture events, may be accomplished by pulse counting. The volume, V, is the sensitive volume of a proportional counter or of an ionization chamber.

The assumption in the foregoing is that slow-neutron absorption by the counter wall is negligible. The validity of the statement depends upon the material and the thickness of the walls. Important aspects of  $BF_3$  proportional counters and pulse chambers can be found in an article by Fowler and Tunnicliffe (6).

A common method to measure R is by collecting the ionization current from the volume V. Since each capture event releases 2,34 mev as the kinetic energy of the alpha and  $Li^7$  particles, and since this energy is lost by ionization and excitation with an energy of about 32.5 ev per ion pair, the ionization current due to neutrons will be (at saturation)

(2-10)

$$I = 1.6 \times 10^{-19} \left( \frac{2.34 \times 10^6}{32.5} \right) VR \left( 1 - \frac{\Delta V}{5V} \right) \text{ Amperes}$$

$\Delta V$  is the volume reduction by moving the chamber walls inward by a distance equal to the range of the alpha in  $BF_3$  gas. The volume correction factor,  $\left( 1 - \frac{\Delta V}{5V} \right)$ , approximately accounts for the capture events occurring near the walls which may not contribute their share of ionization to the gas. If there is a way to subtract that portion of ionization current contributed by gamma and other radiations, the neutron flux can be evaluated by equation (2-9) with the known value R from equation (2-10).

Developed at Oak Ridge National Laboratory, the compensated ionization chamber measures the neutron current alone. This device consists of a pair of ionization chambers, one is filled with dry  $BF_3$  gas and the other is filled with a gas of argon or  $CO_2$  which is insensitive to neutrons. The pressure in the second chamber is adjusted to give an identical ionization current when both chambers are exposed to the same intensity of gamma radiation. Since the  $BF_3$

chamber is sensitive to gamma and neutron radiations, the difference current of the two chambers, as indicated by an electrometer, is the ionization current due to the neutrons. The application of fission chambers to detect neutrons is through the kinetic energy of the fission products. The ionization produced as the fission products are brought to rest is utilized to measure neutron densities.

Fission chambers containing the thermal-fissionable nuclei  $U^{233}$ ,  $U^{235}$ , or  $Pu^{239}$  are efficient thermal-neutron detectors. The large energy released per reaction makes it possible to discriminate against much larger fluxes of gamma rays than with detectors employing  $(n, \alpha)$  or similar reactions. This property makes the fission chambers particularly useful for the measurement of small values of neutron flux which are present in the start up and shut-down of a reactor. The cross sections of  $U^{233}$ ,  $U^{235}$ , and  $Pu^{239}$  follow approximately  $1/v$  dependence so the relationship between reaction rate and thermal flux for boron chambers applies here as a crude approximation.

## 2. Fast Neutron Activation

In most instances the detection of high energy neutrons, energies ranging from 10 kev to about 15 mev, relies on the modified slow neutron detection techniques. A survey of the detection methods for fast neutrons will be given in this section.

Since  $B^{10}$  ( $n, \alpha$ ) has a decreasing cross section for the reaction as neutron energy increases, the sensitivity of the  $B^{10}$  counter is quite small for fast neutrons. Much improvement can be had by surrounding the counter with a neutron moderator so the neutrons are slowed down before entering the counter tube. However, it is found such an arrangement is usually dependent on the neutron energy and the detector-source geometry. These factors make the interpretation of measurement quite difficult.

A detector system known as the "long counter", devised by Hanson and McKibben (7), is essentially independent of neutron energy from 10 kev to 3 mev. The arrangement consists of a paraffin cylinder about 10 inches outer diameter by 12 inches long surrounding a long boron trifluoride proportional counter. The response is flat within 10 percent for the neutron energies between 10 kev and 3 mev.

The application of fission chambers for slow neutron detection was discussed earlier. The underlying principle, threshold reaction, can be applied to detect fast neutrons by suitably selecting fissionable materials with higher threshold energies. Wiegand (8) has described the use of bismuth in a fission chamber which will monitor neutrons with energy greater than 50 mev, the threshold energy for the fission process of bismuth. A list of references (9-12) includes the various fission chamber constructions and characteristics.

The use of a pulse chamber to detect fast neutrons involves the ( $n, p$ ) scattering process. The neutron in the



scattering process transfers part of its energy to the recoil proton and the ionization produced by the protons is a measure of the neutron density.

The hydrogen which is required for the proton recoil counter can be introduced either in a solid or gaseous form. If one assumes that the pulse height produced by each recoil proton is proportional to the proton energy, an expression for the counting rate,  $C(E_n, E_t)$ , for neutrons with energy  $E_n$  is

$$C(E_n, E_t) = \int_{E_t}^{E_n} N_p(E) dE \quad (2-11)$$

where  $E_t$  is the threshold energy of (n,p) reaction and  $N_p(E)$  is the proton recoil energy distribution.

If a region contains  $N_t$  protons in a uniform flux of monoenergetic neutrons with energy  $E_n$ , the number of recoil protons per unit time per unit neutron energy is

$$\frac{N_t \phi_{E_n} \sigma(E_n)}{E_n} \quad (2-12)$$

Since the recoil protons per second per unit energy is the recoil proton energy distribution, the relationship between the counting rate and flux is

$$C(E_n, E_t) = \int_{E_t}^{E_n} \frac{N_t \phi_{E_n} \sigma(E_n) dE}{E_n} = \frac{N_t \phi_{E_n} \sigma(E_n) (E_n - E_t)}{E_n} \quad (2-13)$$

Designs of several different counters of this type can be found in the discussion by Rossi and Staub (9).

For sufficiently large neutron fluxes, the current in an ionization chamber containing hydrogen can be measured.

Again, if the ionization produced in the chamber by each recoil proton is proportional to the proton energy, the idealized saturation current can be written as

$$I = \frac{e}{w} \int_0^{E_n} EN_p(E) dE = \frac{e}{2w} N_t \phi_{E_n} \sigma(E_n) E_n \quad (2-14)$$

In this expression,  $e$  is the electronic charge, and  $w$  is the energy required to produce one ion pair. The factor  $1/2$  is the fraction of the neutron energy imparted to proton assuming isotropic scattering.

Neutron induced reactions which have a threshold energy can be used to detect fast neutrons. A list of some common threshold detectors, their energies, and a discussion of their uses have been given by Cohen (13).

The saturation activity of a threshold detector is given by the well known equation

$$A_s = N_t \int_0^{\infty} \sigma_a(E) \phi(E) dE \quad (2-15)$$

where  $N_t$  is the total number of target atoms in the detector and  $\sigma_a(E)$  is the cross section for activation at energy  $E$ . In the case of the  $P^{31}(n,p)$  and  $S^{32}(n,p)$  reactions, there is a fortunate occurrence of resonances and the cross sections rise quite rapidly and remain rather constant thereafter. In this special case, the actual cross section can be replaced by an idealized cross section,  $\sigma_c$ , whose value is constant from  $E_t$  to infinity. Thus saturation activity is given as

$$A_s = N_t \sigma_c \int_{E_t}^{\infty} \phi(E) dE \quad (2-16)$$

where  $\sigma_c$  is set as the mean value above the threshold. By the use of two foils with threshold energies  $E_{t-1}$  and  $E_{t-2}$ , the total flux in the energy interval  $E_{t-1}$  and  $E_{t-2}$  can be found. Hurst et al (14) have utilized threshold

detectors in this fashion for determining neutron spectra.

The central problem in neutron counting by the use of scintillation detectors is the discrimination against gamma rays. Because of the high density of the scintillation detectors, the secondary electrons released by the gamma rays often dissipate their entire energies in the detectors. Therefore, the scintillator outputs for the gamma rays are often at least as large as those for the neutrons.

Bollinger (15) has described a boron-loaded liquid scintillation counter which minimizes the discriminator problems. The cell containing the scintillator is viewed by four photomultiplier tubes mounted in a circle on one side of the container. The tubes are paired by joining the anodes of the diagonally opposite, the signal from each pair being independently amplified. The electronic system requires coincidence between two amplifier outputs, thus eliminating tube-noise counts. Gamma ray background is minimized by requiring that the sum of the amplifier outputs be in a given pulse-height range.

When a fast neutron enters the liquid scintillator containing boron, two light pulses may be produced, one by the protons scattered by the neutrons and the other upon the capture of the neutrons by the boron. The two pulses should be separated by about  $0.5 \mu\text{sec}$ , the time required for the capture of neutron in the boron. Since the individual pulses are quite short (around  $5 \times 10^{-9}$  sec), they can be resolved. Thus the fast neutron can be identified by the appearance of two pulses. By the use of a delayed coincidence circuit, the fast neutrons can be separated from the gamma rays and the slow neutrons, each of which gives one signal pulse.

An ingenious application of organic scintillators has been developed (16) which is insensitive to gamma radiation and for which the detection efficiency is strongly dependent on neutron energy. The counting medium consists of spheres

of a plastic scintillator immersed in nonhydrogeneous optically inert material (glass or trifluorochloroethylene liquid). The sphere diameter is chosen large enough that, for a particular neutron energy, most recoil protons dissipate their energy within the scintillator. However, it must be small enough to prevent the pulses of maximum size caused by gamma rays from being in the same pulse-height range as those due to the neutrons.

Nuclear emulsions have been found satisfactory for neutron energy distribution measurements of neutrons in the energy range from about 0.5 to 15 mev. The lower limit arises since the track ranges become too short for accurate measurements while the upper limit comes from a practical limit of emulsion thickness.

Several techniques have been developed for the measurement of neutron energy and spectra through the use of nuclear emulsions. Extensive review of the nuclear emulsion techniques has been given by Rosen (17). The choice of method depends on several factors such as the degree of collimation of the neutrons, the energy region in which the measurement is required, and the facilities and time available for measuring the tracks.

One technique commonly used is that of measuring the range of proton recoils in the emulsion within a small angle from the forward direction. This technique requires the knowledge of the direction of the primary neutrons. Through the use of the range-energy relationship, readily attainable through the suppliers of the emulsions, the energies associated with the proton recoils can be determined.

A considerable amount of work has been devoted to the establishment of precise range-energy relationship for various types of nuclear emulsions (18). Since changes in emulsion composition affect range measurement, it is a common practice to calibrate emulsions under the conditions

of exposure and development to be employed in the experiment.  
This can be done by using particles of known range.

### III THEORY AND EXPERIMENTAL PROCEDURE

A detector placed in a uniform neutron flux,  $\phi$ , has a rate of change of radioactive atoms given by the difference between the rate of radioactive formation and the rate of decay, assuming negligible loss due to neutron capture. If the decay constant is  $\lambda$ , the rate of change of radioactive atoms,  $\frac{dN}{dt}$ , is

$$\frac{dN}{dt} = \sigma_a N_d S_d \phi - \lambda N \quad (3-1)$$

The rate of radioactive formation is  $\sigma_a N_d S_d \phi$  where  $\sigma_a$  is the activation cross section of the detector,  $N_d$  and  $S_d$  are the molecular surface density and the surface area of the detector respectively. It follows from equation (3-1) that  $N$ , the number of radioactive atoms present at time  $t$  is.

$$N = \frac{\sigma_a N_d S_d \phi}{\lambda} (1 - e^{-\lambda t}) \quad (3-2)$$

where time is measured from the commencement of the irradiation.

When a detector is irradiated for a duration of  $t_1$ , the number of radioactive atoms decaying for a length of time  $T$  after removal from the flux for a period of  $t_2$  is

$$N_T = \frac{\sigma_a N_d S_d \phi}{\lambda} (1 - e^{-\lambda t_1}) (1 - e^{-\lambda T}) e^{-\lambda t_2} \quad (3-3)$$

If the counter efficiency is  $e_c$  and the fractional counts due to the geometry is  $e_g$ , then the total count,  $C$ , registered for the interval  $T$  is

$$C = e_c e_g N_T \quad (3-4)$$

For a particular counter with a constant counting geometry it is evident that the flux  $\phi$ , is directly proportional

to the registered counts after the correction. If the absolute flux is known for any one count, the absolute flux profile can be obtained.

In 19W loading, (19 represents the loading arrangement and W stands for the water reflector) 14 copper wires of gauge number 14, each 30 inches long, were positioned into the center of the fuel elements. A plastic holder for the copper wire was designed to rest between the top edges of any two fuel plates. The holders and the wires, each numbered for identification, were lowered into the fuel elements by nylon strings, positioned as shown in figure 2a. The reactor was brought to a power level of 10 kilowatts at a constant period and operated for 20 minutes as the total duration of the irradiation. The contribution to the radioactivity,  $N'$ , while the reactor is approaching 10 kilowatts can be represented by

$$\frac{dN'}{dt} = \sigma_a N_d S_d \phi_0 e^{\frac{t}{T}} - \lambda N' \quad (3-5)$$

where  $\phi_0$  is the flux when the reactor is critical,  $T$  is the reactor period, and  $t$  is the time between critical and final steady power of the reactor. As the calculation shows in appendix 2, the contribution to the radioactivity is negligible and is well within the error of the National Bureau of Standards flux source.

In order to minimize the radiation hazard, the radioactive wires were allowed to decay at least 4 half lives before handling. Counting was done at two inch intervals for one minute periods starting at the 30 inch mark of the wire, a position corresponding to the bottom portion of the fuel element. As the water reflecting wing at the top appears as part of the 2 inch interval count, an extra reading at the 29th inch was necessary to locate the reflecting wing at the bottom. Counting was done with the G-M tube, model 10106, by Radiation Counter Lab, Inc. It was attached to a scalar model DS-5B by Technical Associated and operated at

A1	A2	A3	A4	A5	A6	A7	A8	A9
B1	B2	B3	B4	B5	B6	B7	B8	B9
C1	C2	C3	C4	C5	C6	C7	C8	C9
D1	D2	D3	D4	D5	D6	D7	D8	D9
E1	E2	E3	E4	E5	E6	E7	E8	E9
F1	F2	F3	F4	F5	F6	F7	F8	F9

FIGURE 1 a CORE ARRANGEMENT



				S				
			F-12	F-8	HR-1			
		F-22	C-1	F-15	C-4	F-18		
		F-5	C-2	F-13	C-3	F-3		
		F-2	F-21	F-10	F-7	F-14		

FIGURE 1b SOURCE, S, AND FUEL POSITIONS

A									
B									
C			12	13	14				
D		9		10		11			
E		6		7		8			
F		1	2	3	4	5			
	1	2	3	4	5	6	7	8	9

FIGURE 2a WIRE POSITIONS FOR 19W

A									
B									
C			12	16	14				
D		9		10		11			
E		6		7		8			
F		1	2	3	4	5			
	1	2	3	4	5	6	7	8	9

FIGURE 2b WIRE POSITIONS FOR 19T

1320 volts, the middle of the G-M tube plateau. The counting arrangement with the lead bricks as shield provides constant geometry and is arranged as in figure 3.

Four gold foils, irradiated in the thermal neutron pile of the National Bureau of Standards, were used as the absolute neutron flux standard for the calibration. Using gold foils of known masses, two foils were positioned inside each fuel element at core position F-6 and F-4 at a known distance along the length of the element. These foils were irradiated for ten minutes at a reactor power of 10 watts. Subsequently four identical foils with cadmium covers were irradiated under the same conditions. The difference between the saturation counts of the bare and cadmium covered foils is proportional to the thermal neutron flux. Saturation count is the number of radioactive atoms present when the decay time is zero and the sample is irradiated for an infinite time. A sample calculation to determine the absolute flux at a point in the reactor is done in appendix 3.

A plastic strip, 1 1/4 inches by 32 inches, was used as the foil holder. Six holes spaced 4 inches apart starting from the 26th inch were drilled to fit the round cadmium covers. Commercially obtainable black electrical tape was employed to hold the foils and the covers secure. Again, nylon string was used to lower the plastic strip into the fuel element. It was found that lead weights must be added to the strip to make positioning possible.

A scintillation tube positioned inside a lead shield was used to count the radioactivity of the gold foils. A plateau run indicated the best operating voltage is 1120 volt. For reproducible geometry, shelf number 1 of the standard counting set-up was used for all the foil counting. Fifteen minute counts were taken for all the foils except the standard foils where counting was done for a period of 50 minutes. The foil counting set-up is arranged as in figure 4.



FIGURE 3 WIRE COUNTING GEOMETRY

- A: Copper Wire
- B: G-M Tube
- C: Lead Shield
- D: Scalar



FIGURE 4 FOIL COUNTING GEOMETRY

- A: Gold Foil, Shelf, and Counting Stand
- B: Scintillation Tube
- C: Lead Shield
- D: Scalar

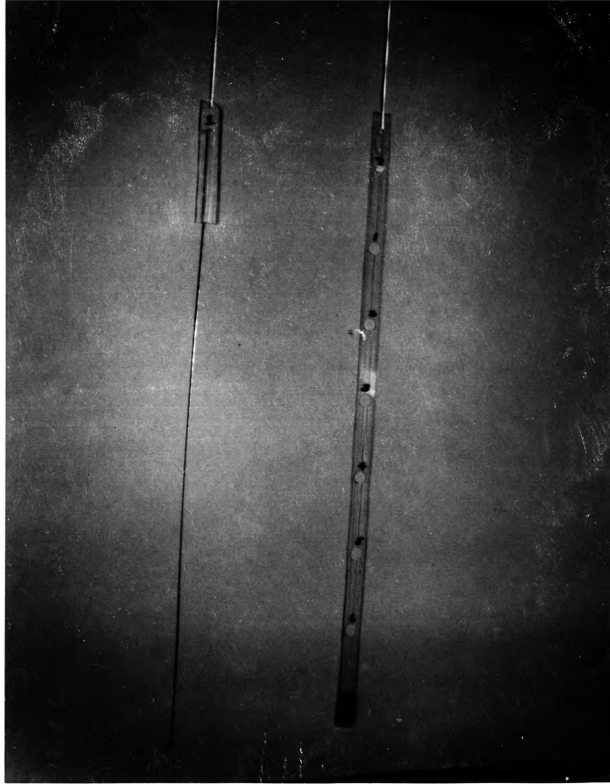


FIGURE 5 FOIL AND WIRE HOLDERS

The same procedure was used for the 19T core arrangement where the reactor is moved against the thermal column, The data together with the correction can be found on Tables I and IV.

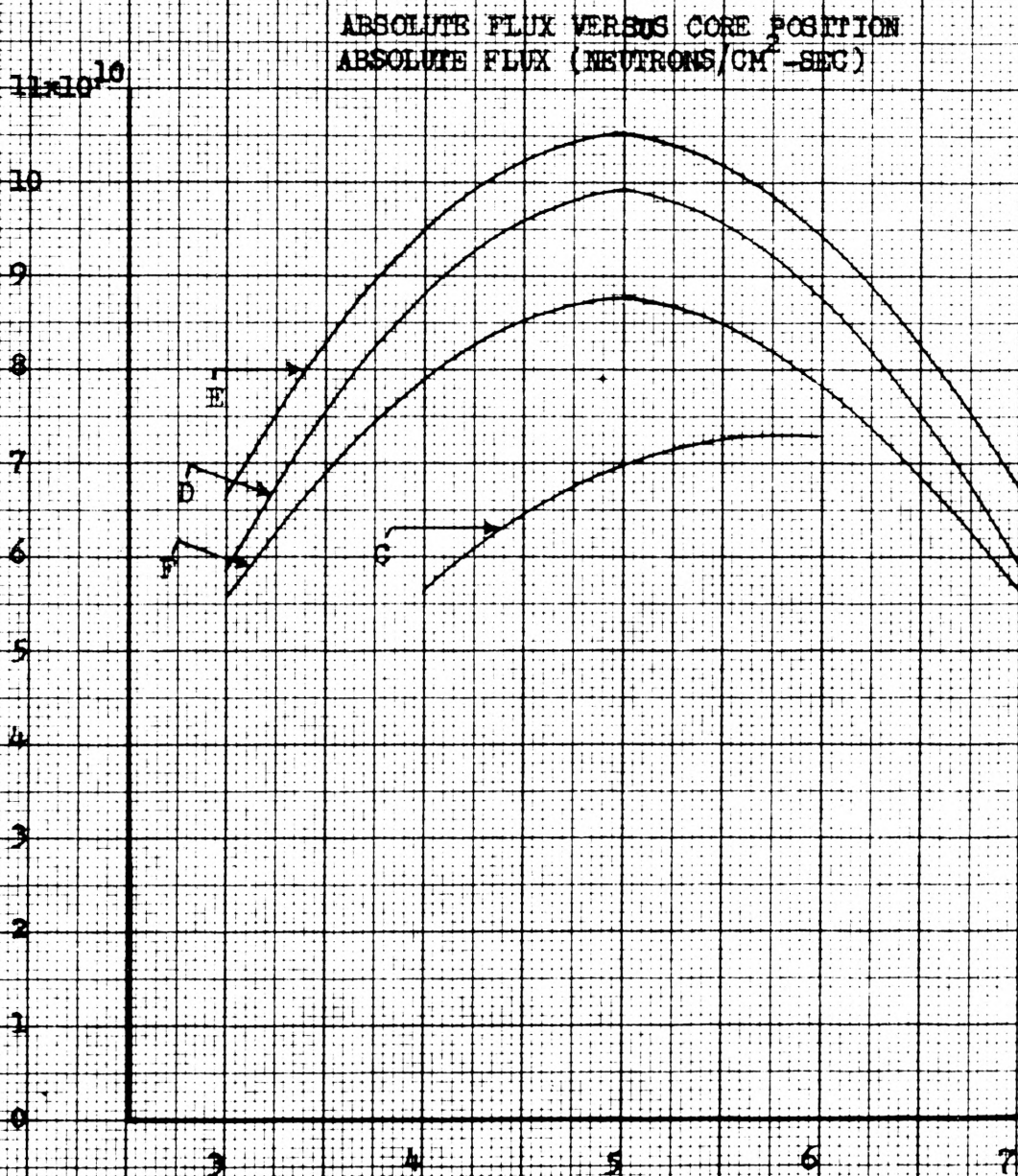


FIGURE 6 FLUX DISTRIBUTION OF THE CORE FOR 19W



$8 \times 10^3$

RELATIVE FLUX (SATURATION COUNTS) VERSUS FUEL LENGTH (INCHES)

7

6

5

4

3

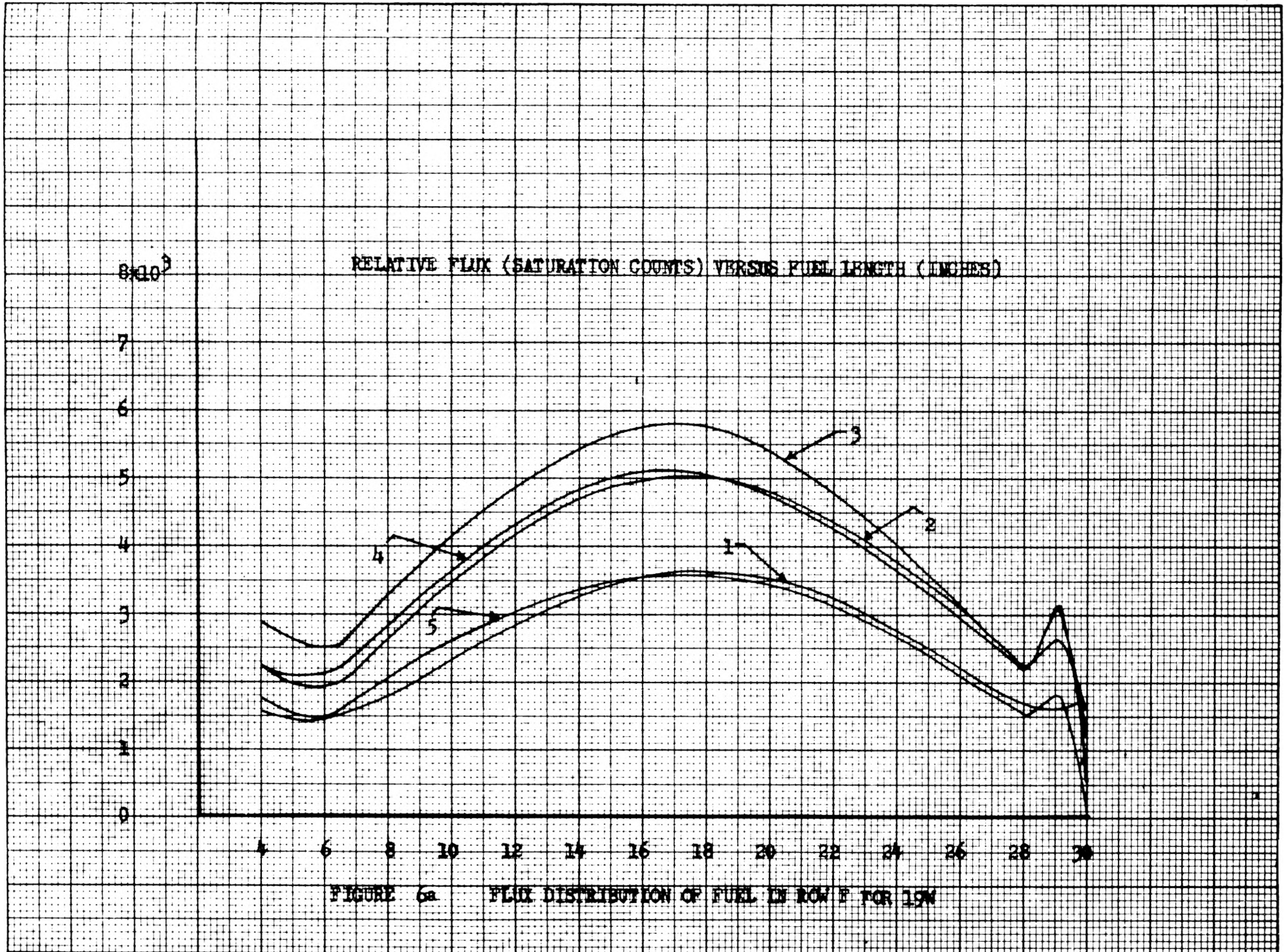
2

1

0

4 6 8 10 12 14 16 18 20 22 24 26 28 30

FIGURE 6a FLUX DISTRIBUTION OF FUEL IN ROW F FOR 194



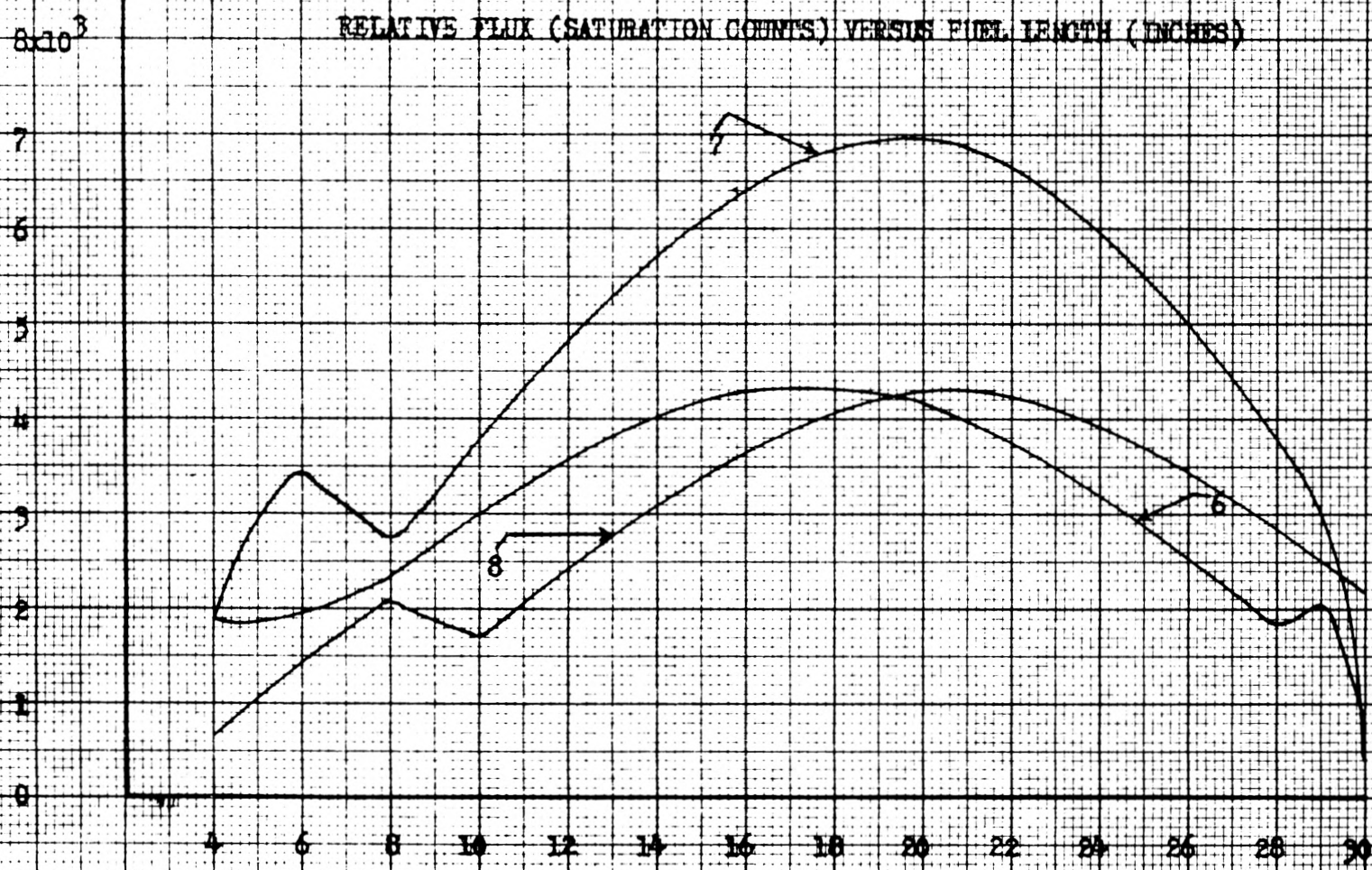


FIGURE 6b FLUX DISTRIBUTION OF FUEL IN ROW E FOR 19M

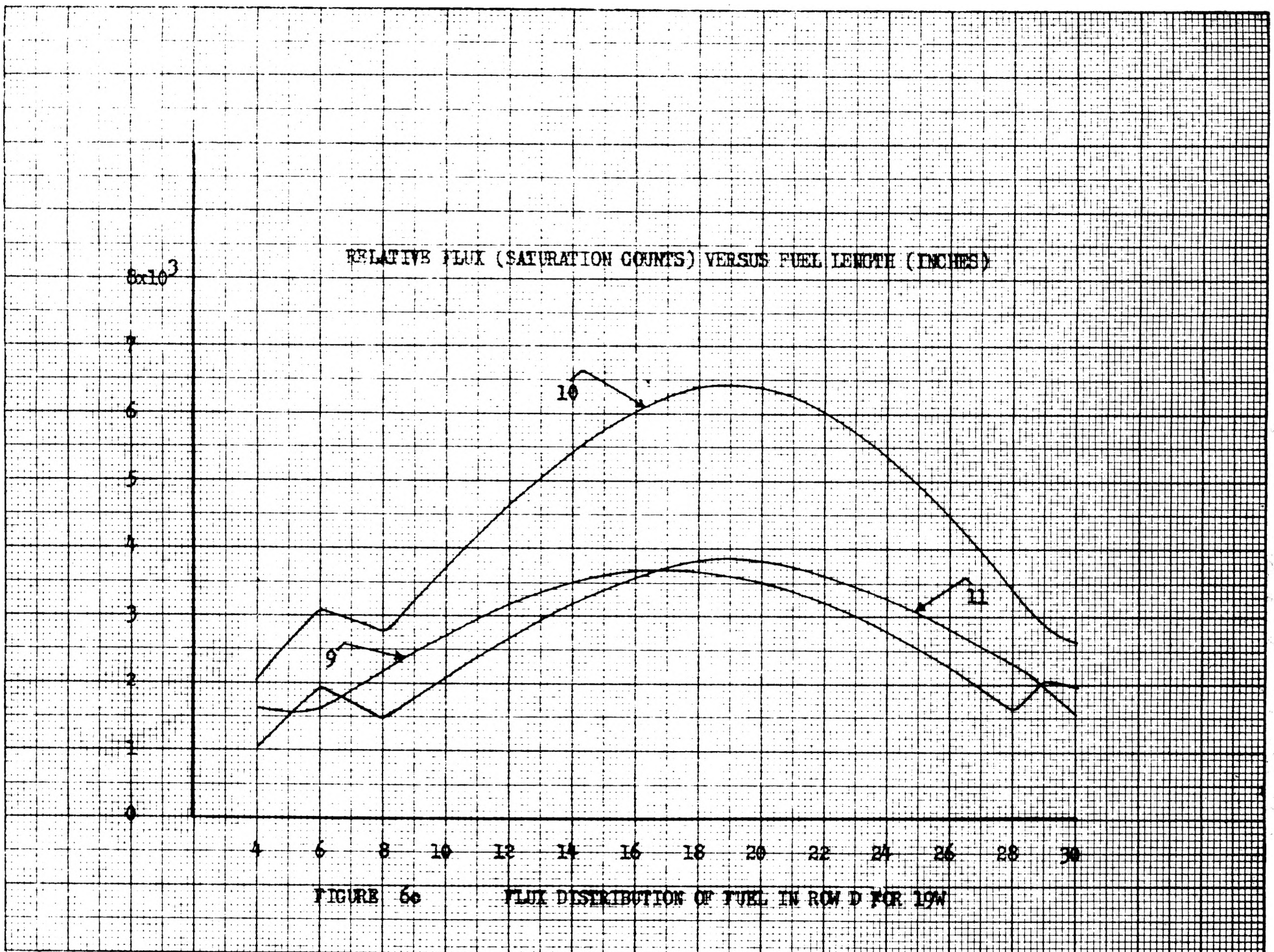


FIGURE 60 FLUX DISTRIBUTION OF FUEL IN ROW D FOR 19W

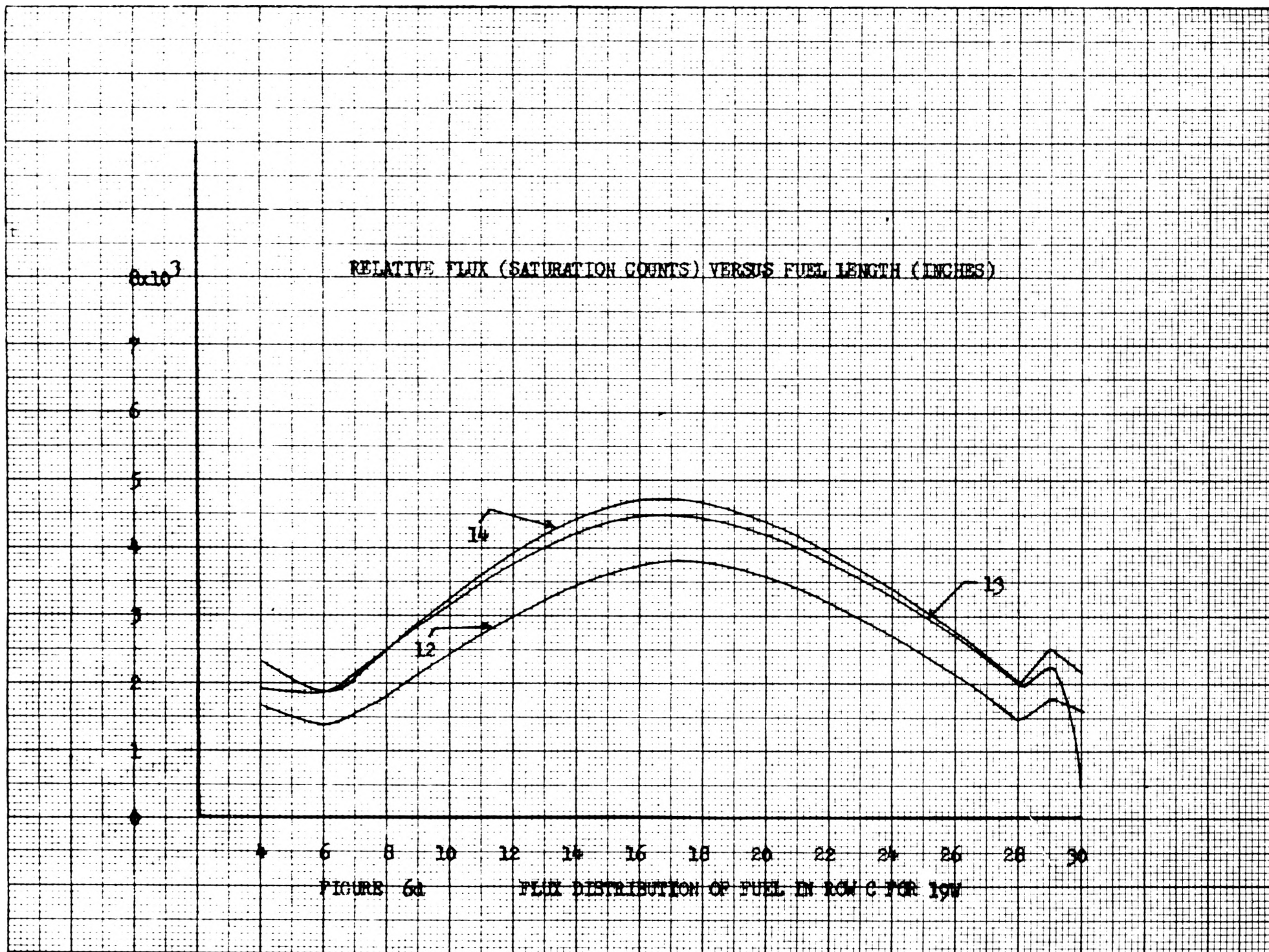


TABLE I WIRE ACTIVATION FOR 19W

## General Information :

Irradiation date : May 5, 1962  
 Reactor power : 10 kilowatts  
 Critical time : 10:30 A.M.  
 Level time : 10:41 A.M.  
 Period of the reactor : 70 seconds  
 Scram time : 11:01 A.M.  
 Irradiation time : 20 minutes

## Wire No. 1

Position (inches)	N(counts per min.)	$t_2$ (decay <sup>2</sup> time)	$e^{-\lambda t_2}$	$\frac{N}{e^{-\lambda t_2}}$
30	1261	5 hr. 13 min.	.7555	1669
29	1567	" 14 "	.7548	2077
28	1287	" 16 "	.7535	1708
26	1710	" 17 "	.7528	2272
24	2092	" 18 "	.7521	2782
22	2292	" 19 "	.7514	3050
20	2648	" 20 "	.7508	3527
18	2736	" 21 "	.7500	3648
16	2657	" 22 "	.7494	3546
14	2461	" 23 "	.7487	3287
12	2157	" 24 "	.7480	2884
10	1803	" 25 "	.7473	2413
8	1327	" 27 "	.7459	1779
6	1079	" 28 "	.7453	1448
4	1146	" 32 "	.7426	1543
Average				2799

## Wire No. 2

Position (inches)	N(counts per min.)	$t_2$ (decay <sup>2</sup> time)	$e^{-\lambda t_2}$	$\frac{N}{e^{-\lambda t_2}}$
30	1368	3 hr. 4 min.	.8481	1613
29	2291	" 6 "	.8466	2707
28	1907	" 7 "	.8458	2254
26	2562	" 9 "	.8443	3034
24	3222	" 10 "	.8435	3820
22	3769	" 11 "	.8428	4473
20	3981	" 12 "	.8420	4728
18	4192	" 13 "	.8413	4984
16	4201	" 15 "	.8397	5004
14	4093	" 17 "	.8382	4884
12	3538	" 18 "	.8374	4225
10	2881	" 19 "	.8367	3443
8	2272	" 20 "	.8359	2718
6	1561	" 21 "	.8352	1869
4	1845	" 22 "	.8344	2211
Average				3947

## Wire No. 3

30	476	2 hr. 46 min.	.8618	552
29	2678	" 47 "	.8611	3110
28	1923	" 49 "	.8595	2237
26	2690	" 50 "	.8588	3132
24	3439	" 51 "	.8580	4008
22	3989	" 52 "	.8572	4653
20	4577	" 53 "	.8565	5344

## Wire No. 3

Position (inches)	N(counts per min.)	$t_2$ (decay time)	$e^{-\lambda t_2}$	$\frac{N}{e^{-\lambda t_2}}$
18	4839	2 hr. 54 min.	.8557	5655
16	4733	" 56 "	.8542	5541
14	4697	" 57 "	.8534	5503
12	4145	" 58 "	.8527	4862
10	3589	" 59 "	.8519	4212
8	2785	3 hr.	.8512	3272
6	2080	1 min.	.8504	2445
4	2460	2 "	.8496	2895
Average				4415

## Wire No. 4

30	1165	45 "	.9604	1213
29	2497	47 "	.9587	2604
28	2160	46 "	.9596	2251
26	2844	48 "	.9579	2969
24	3558	49 "	.9570	3718
22	3947	50 "	.9562	4128
20	4357	51 "	.9553	4560
18	4759	52 "	.9545	4986
16	5001	53 "	.9536	5244
14	4527	54 "	.9528	4751
12	4181	56 "	.9511	4395
10	3554	58 "	.9494	3743
8	2656	59 "	.9485	2800

## Wire No. 4

Position (inches)	N(counts per min.)	$t_2$ (decay <sup>2</sup> time)	$e^{-\lambda t_2}$	$\frac{N}{e^{-\lambda t_2}}$
6	1124	22 hr. 13 min.	.3031	3708
4	1012	" 14 "	.3029	3341
Average				6721

## Wire No. 5

30	266	2 hr. 30 min.	.8740	304
29	2523	" 31 "	.8733	2890
28	3162	" 32 "	.8725	3624
26	3995	" 33 "	.8717	4583
24	4584	" 35 "	.8702	5268
22	4920	" 36 "	.8694	5659
20	5047	" 37 "	.8687	5810
18	4775	" 37 "	.8671	5506
16	4728	" 40 "	.8664	5457
14	4061	" 41 "	.8656	4691
12	3177	" 42 "	.8649	3674
10	2530	" 43 "	.8641	2928
8	1659	" 45 "	.8626	1924
6	2496	" 46 "	.8618	2897
4	1549	" 47 "	.8610	1800
Average				4393

## Wire No. 6

30	1898	5 hr. 18 min.	.7521	2524
29	2951	" 19 "	.7513	3928
28	3590	" 20 "	.7508	4782



## Wire No. 6

Position (inches)	N(counts per min.)	$t_2$ (decay <sup>2</sup> time)	$e^{-\lambda t_2}$	$\frac{N}{e^{-\lambda t_2}}$
24	2830	10 min.	.8901	3179
22	3322	11 "	.8893	3736
20	3557	13 "	.8877	4008
18	3658	14 "	.8869	4125
16	3793	15 "	.8861	4281
14	3492	16 "	.8853	3945
12	3180	17 "	.8845	3599
10	2706	19 "	.8829	3065
8	1959	20 "	.8821	2221
6	1712	21 "	.8813	1943
4	1644	22 "	.8804	1867
Average				3337

## Wire No. 7

30	332	3 hr. 24 min.	.8329	398
29	2776	" 25 "	.8321	3336
28	3327	" 27 "	.8306	4006
26	4325	" 28 "	.8298	5212
24	4936	" 29 "	.8290	5954
22	5482	" 30 "	.8283	6619
20	5788	" 31 "	.8276	6994
18	5622	" 32 "	.8268	6800
16	5289	" 34 "	.8254	6408
14	4886	" 35 "	.8247	5925

## Wire No. 7

Position (inches)	N(counts per min.)	$t_2$ (decay <sup>2</sup> time)	$e^{-\lambda t_2}$	$\frac{N}{e^{-\lambda t_2}}$
12	4041	3 hr. 36 min.	.8240	4905
10	3083	" 37 "	.8232	3745
8	2242	" 39 "	.8218	2728
6	2801	" 40 "	.8211	3418
4	1475	" 41 "	.8203	1798
Average				5288

## Wire No. 8

30	2123	25 min.	.9776	2172
29				
28	2932	26 "	.9767	3002
26	3311	28 "	.9749	3396
24	3737	29 "	.9740	3837
22	4144	30 "	.9731	4259
20	3986	31 "	.9723	4100
18	3925	32 "	.9714	4041
16	3576	34 "	.9698	3688
14	3002	35 "	.9689	3098
12	2435	36 "	.9681	2516
10	1641	37 "	.9672	1696
8	2002	38 "	.9664	2072
6	1443	39 "	.9655	1494
4	627	41 "	.9638	650
Average				3390

## Wire No. 9

Position (inches)	N(counts per min.)	$t_2$ (decay time)	$e^{-\lambda t_2}$	$\frac{N}{e^{-\lambda t_2}}$
30	1523	4 hr. 52 min.	.7699	1978
29	1595	" 53 "	.7692	2073
28	1248	" 55 "	.7678	1625
26	1763	" 56 "	.7672	2298
24	2145	" 57 "	.7665	2798
22	2485	" 58 "	.7658	3245
20	2530	" 59 "	.7651	3307
18	2793	5 hr. 1 min.	.7637	3658
16	2835	" 2 "	.7630	3716
14	2708	" 3 "	.7624	3552
12	2456	" 5 "	.7610	3227
10	2102	" 6 "	.7603	2764
8	1699	" 7 "	.7596	2237
6	1186	" 8 "	.7589	1562
4	1219	" 10 "	.7576	1609
Average				2948

## Wire No. 10

30	2289	2 hr. 24 min.	.8788	2605
29	2446	" 25 "	.8780	3421
28	2889	" 26 "	.8772	3293
26	4076	" 28 "	.8756	4655
24	4660	" 33 "	.8717	5345
22	5220	" 34 "	.8710	5993

## Wire No. 10

Position (inches)	N(counts per min.)	$t_2$ (decay time)	$e^{-\lambda t_2}$	$\frac{N}{e^{-\lambda t_2}}$
20	5585	2 hr. 35 min.	.8702	6401
18	5643	" 36 "	.8694	6490
16	5263	" 37 "	.8687	6058
14	4643	" 38 "	.8679	5350
12	4070	" 40 "	.8664	4698
10	3356	" 41 "	.8656	3877
8	2369	" 42 "	.8649	2740
6	2668	" 43 "	.8641	3087
4	1773	" 44 "	.8634	2053
Average				4989

## Wire No. 11

30	1440	1 hr. 6 min.	.9426	1528
29	1792	" 8 "	.9409	1905
28	2152	" 9 "	.9401	2289
26	2687	" 10 "	.9392	2861
24	3213	" 11 "	.9384	3424
22	3342	" 12 "	.9375	3565
20	3591	" 13 "	.9367	3834
18	3551	" 14 "	.9358	3795
16	3349	" 16 "	.9341	3585
14	3003	" 17 "	.9333	3218
12	2519	" 18 "	.9324	2702
10	1883	" 19 "	.9316	2021

## Wire No. 11

Position (inches)	N(counts per min.)	$t_2$ (decay <sup>2</sup> time)	$e^{-\lambda t_2}$	$\frac{N}{e^{-\lambda t_2}}$
8	1376	1 hr. 20 min.	.9308	1479
6	1820	" 21 "	.9299	1957
4	950	" 23 "	.9282	1023
Average				2967

## Wire No. 12

30	1224	5 hr. 35 min.	.7407	1652
29	1345	" 36 "	.7400	1816
28	1104	" 38 "	.7387	1494
26	1416	" 40 "	.7374	1920
24	2077	" 41 "	.7368	2819
22	2306	" 42 "	.7361	3132
20	2478	" 43 "	.7355	3369
18	2800	" 45 "	.7342	3814
16	2671	" 46 "	.7335	3641
14	2577	" 47 "	.7329	3517
12	2213	" 48 "	.7322	3022
10	1828	" 49 "	.7316	2498
8	1344	" 50 "	.7309	1838
6	1014	" 51 "	.7303	1388
4	1249	" 52 "	.7296	1712
Average				2822

## Wire No. 13

Position (inches)	N(counts per min.)	$t_2$ (decay <sup>2</sup> time)	$e^{-\lambda t_2}$	$\frac{N}{e^{-\lambda t_2}}$
30	1976	1 hr. 27 min.	.9248	2137
29	2319	" 28 "	.9239	2510
28	1892	" 29 "	.9231	2050
26	2431	" 30 "	.9222	2636
24	3095	" 32 "	.9207	3362
22	3553	" 33 "	.9198	3863
20	3857	" 34 "	.9190	4198
18	4082	" 35 "	.9182	4446
16	4188	" 36 "	.9174	4565
14	3939	" 37 "	.9166	4297
12	3502	" 38 "	.9158	3824
10	2871	" 40 "	.9142	3140
8	2275	" 41 "	.9134	2491
6	1709	" 42 "	.9126	1872
4	2112	" 43 "	.9118	2342
Average				3529

## Wire No. 14

30	158	1 hr. 45 min.	.9102	173
29	2071	" 46 "	.9094	2277
28	1814	" 47 "	.9086	1996
26	2574	" 50 "	.9062	2840
24	3209	" 51 "	.9054	3544
22	3471	" 52 "	.9046	3837
20	3920	" 54 "	.9030	4341

Wire No. 14

Position (inches)	N(counts per min.)	$t_2$ (decay <sup>2</sup> time)	$e^{-\lambda t_2}$	$\frac{N}{e^{-\lambda t_2}}$
18	4183	1 hr. 55 min.	.9022	4637
16	4267	" 56 "	.9014	4734
14	3938	" 57 "	.9006	4373
12	3653	" 58 "	.8998	4060
10	3070	2 hr.	.8981	3418
8	2225	" 1 min.	.8973	2480
6	1678	" 2 "	.8965	1871
4	1731	" 3 "	.8957	1932
Average				3662

TABLE II GOLD FOIL ACTIVATION FOR 19W

## A. Bare Gold Foils

## General Information :

Irradiation date : May 25, 1962

Reactor power : 10 watts

Critical time : 10:51 A.M.

Level time : 10:55:30 A.M.

Period of the reactor : 47.5 seconds

Scram time : 11:05:30 A.M.

Irradiation time : 10 minutes

Core Position	Vertical Position (inches)	Foil Mass (grams)	N(counts per 15 min.)	$t_2$ (decay <sup>2</sup> time)	Saturation Counts
F-4	18	.1082	134,141	3 days 16 min.	$6.115 \times 10^{10}$
F-4	14	.1084	127,988	3 days	$5.818 \times 10^{10}$
F-6	18	.1085	124,841	3 days 33 min.	$5.708 \times 10^{10}$
F-6	14	.1090	123,845	3 days 49 min.	$5.679 \times 10^{10}$



## B. Cadmium Covered Gold Foils

### General Information :

Irradiation date : May 25, 1962

Reactor power : 10 watts

Critical time : 1:38 P.M.

Level time : 1:43:20 P.M.

Period of the reactor : 53 seconds

Scram time : 1:53:20 P.M.

Irradiation time : 10 minutes

Core Position	Vertical Position (inches)	Foil Mass (grams)	N(counts per 15 min.)	$t_2$ (decay <sup>2</sup> time)	Saturation Counts
F-4	18	.1082	85,888	5 hr. 2 min.	$1.867 \times 10^{10}$
F-4	14	.1084	78,873	2 hr. 28 min.	$1.704 \times 10^{10}$
F-6	18	.1085	83,217	1 hr. 53 min.	$1.787 \times 10^{10}$
F-6	14	.1090	85,942	2 hr. 46 min.	$1.863 \times 10^{10}$

TABLE III NATIONAL BUREAU OF STANDARDS GOLD FOILS

## General Information :

Irradiation start : 9:55 A.M. EST, May 7, 1962

Irradiation end : 2:15 P.M. EST, May 14, 1962

Irradiation time : 7 days 4 hours and 20 minutes

Standard pile flux :  $4.23 \times 10^3$  neutrons per  $\text{cm}^2$  per second (  $\pm 1.5$  per cent )

Foil Mass (grams)	N(counts per 50 min.)	$t_2$ (decay <sup>2</sup> time)	Saturation Counts
.1168	6,599	2 days 18 hr. 21 min.	$1.7972 \times 10^6$
.1122	6,514	2 days 19 hr. 24 min.	$1.7941 \times 10^6$
.1119	6,396	2 days 20 hr. 18 min.	$1.7786 \times 10^6$
.1078	6,131	2 days 21 hr. 15 min.	$1.7222 \times 10^6$

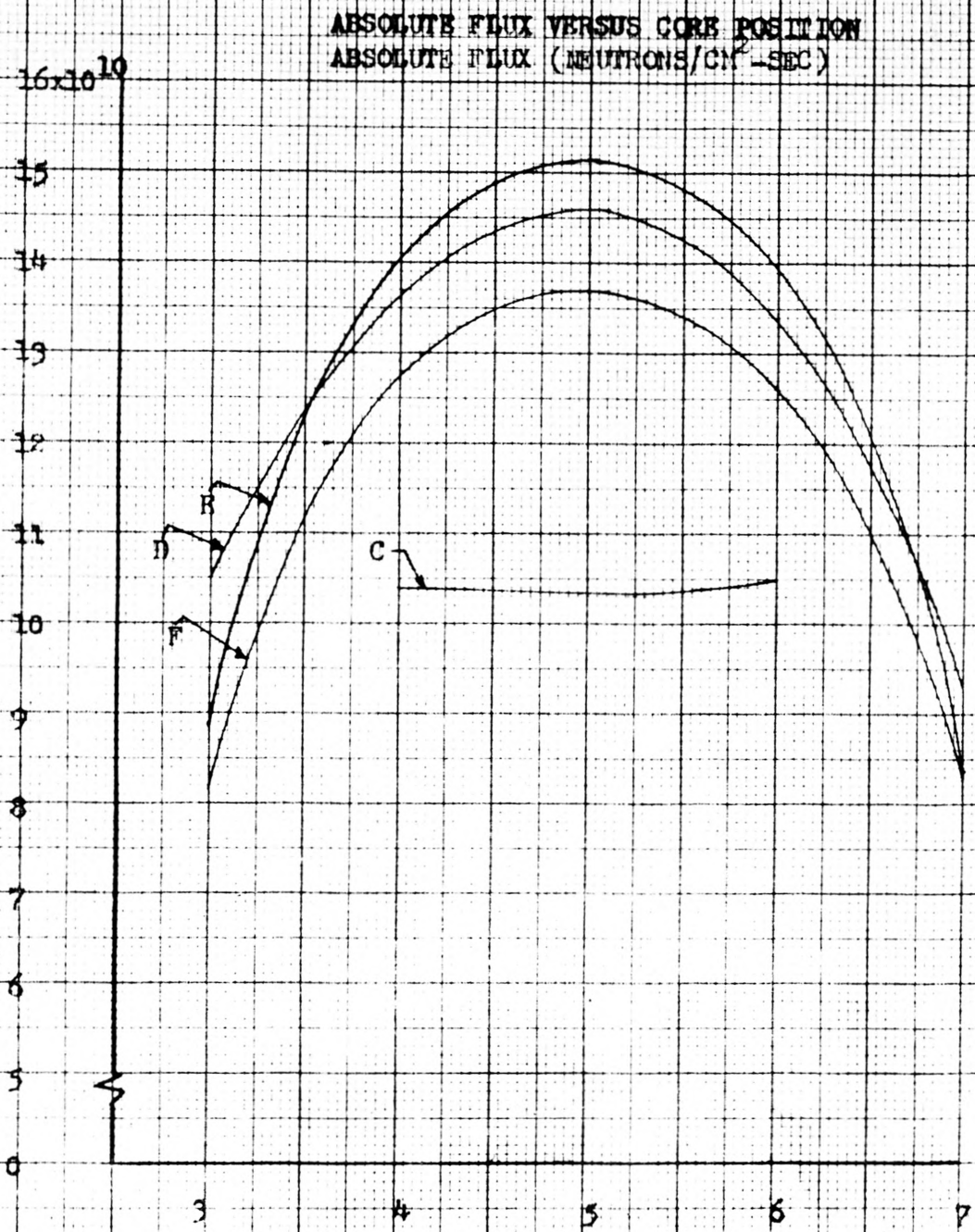


FIGURE 7 FLUX DISTRIBUTION OF THE CORE FOR 12T

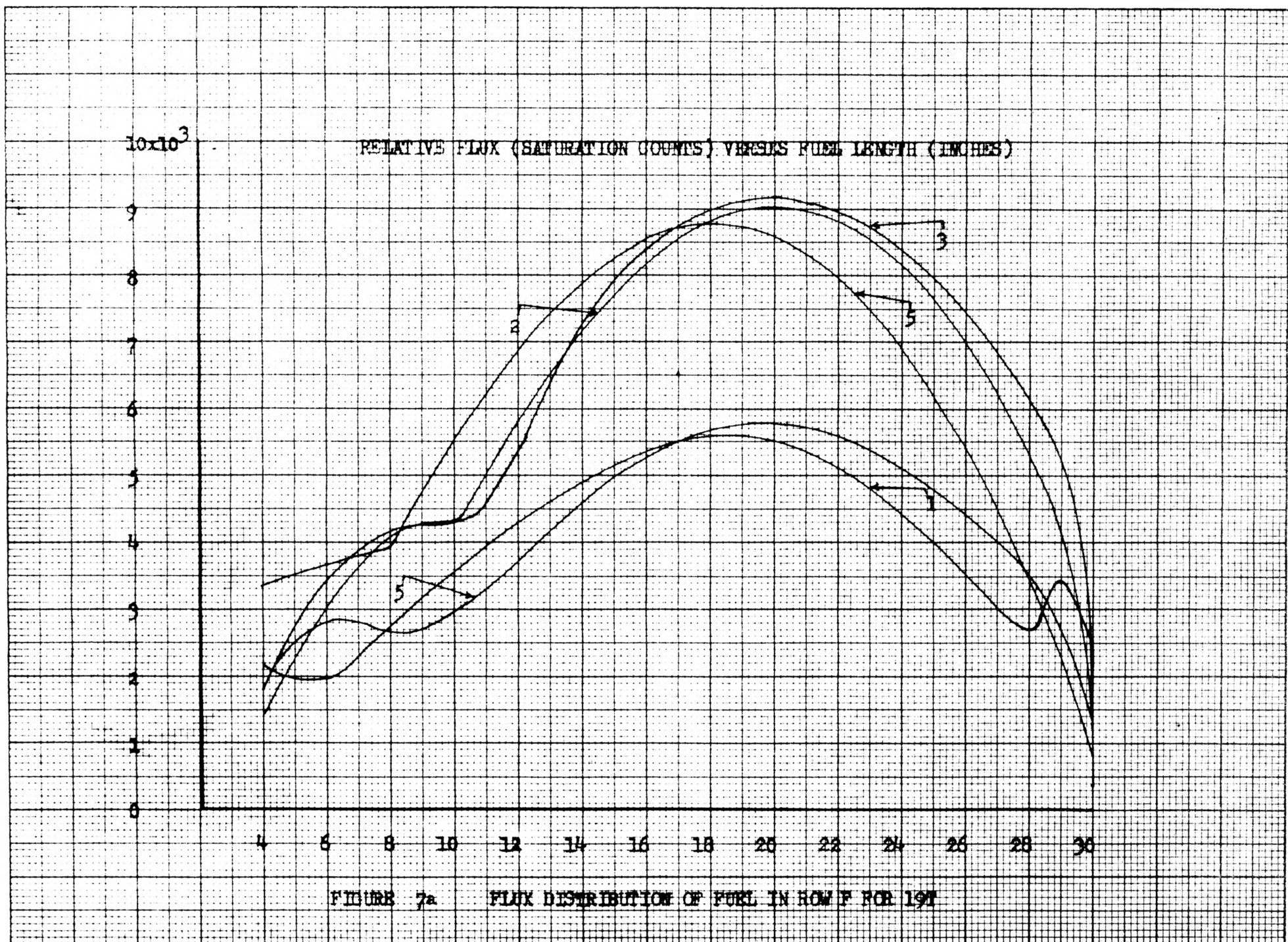
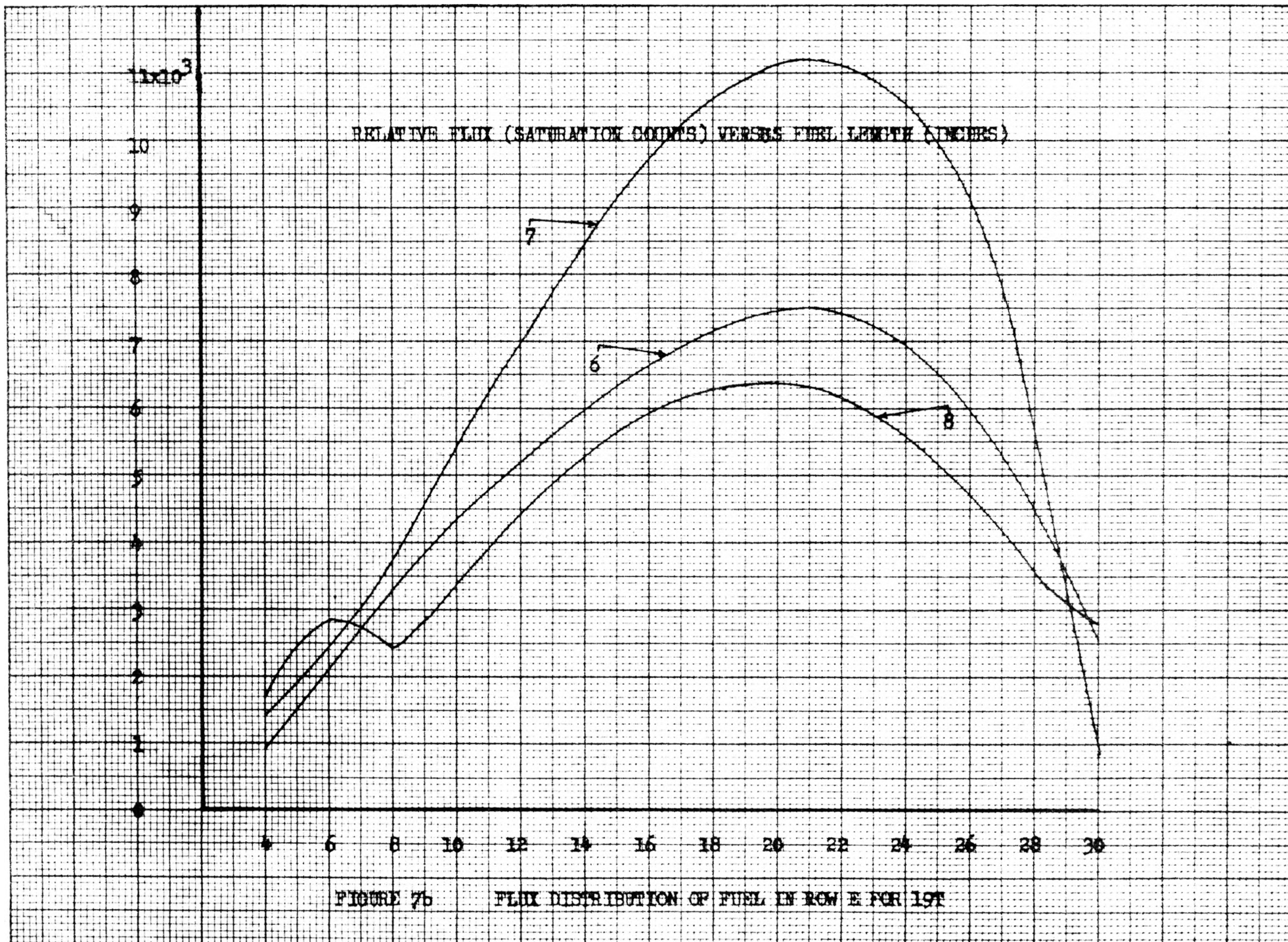


FIGURE 7a FLUX DISTRIBUTION OF FUEL IN ROW F FOR 19T



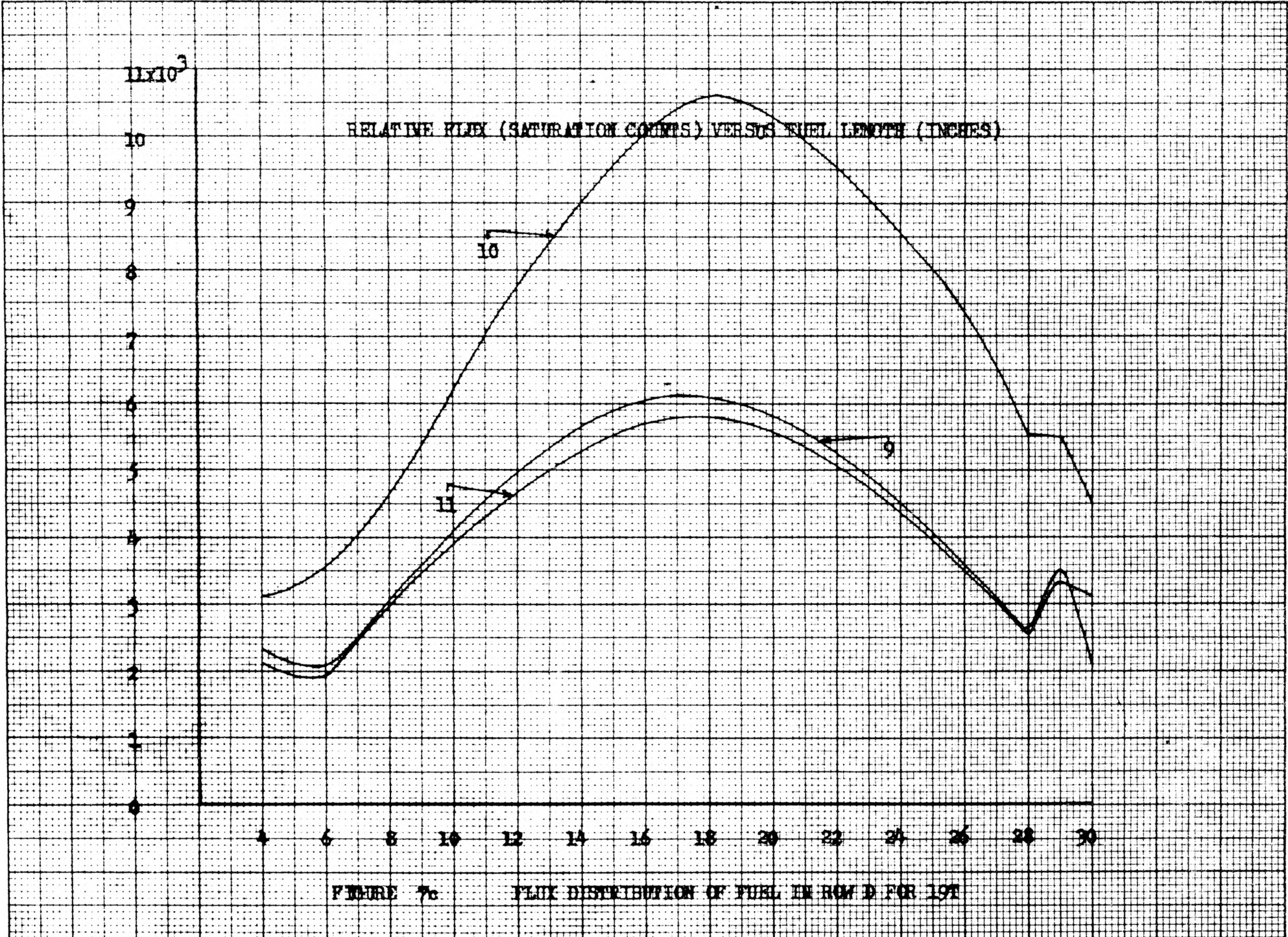


FIGURE 7c FLUX DISTRIBUTION OF FUEL IN ROW D FOR 19T

$10 \times 10^3$

RELATIVE FLUX (SATURATION COUNTS) VERSUS FUEL LENGTH (INCHES)

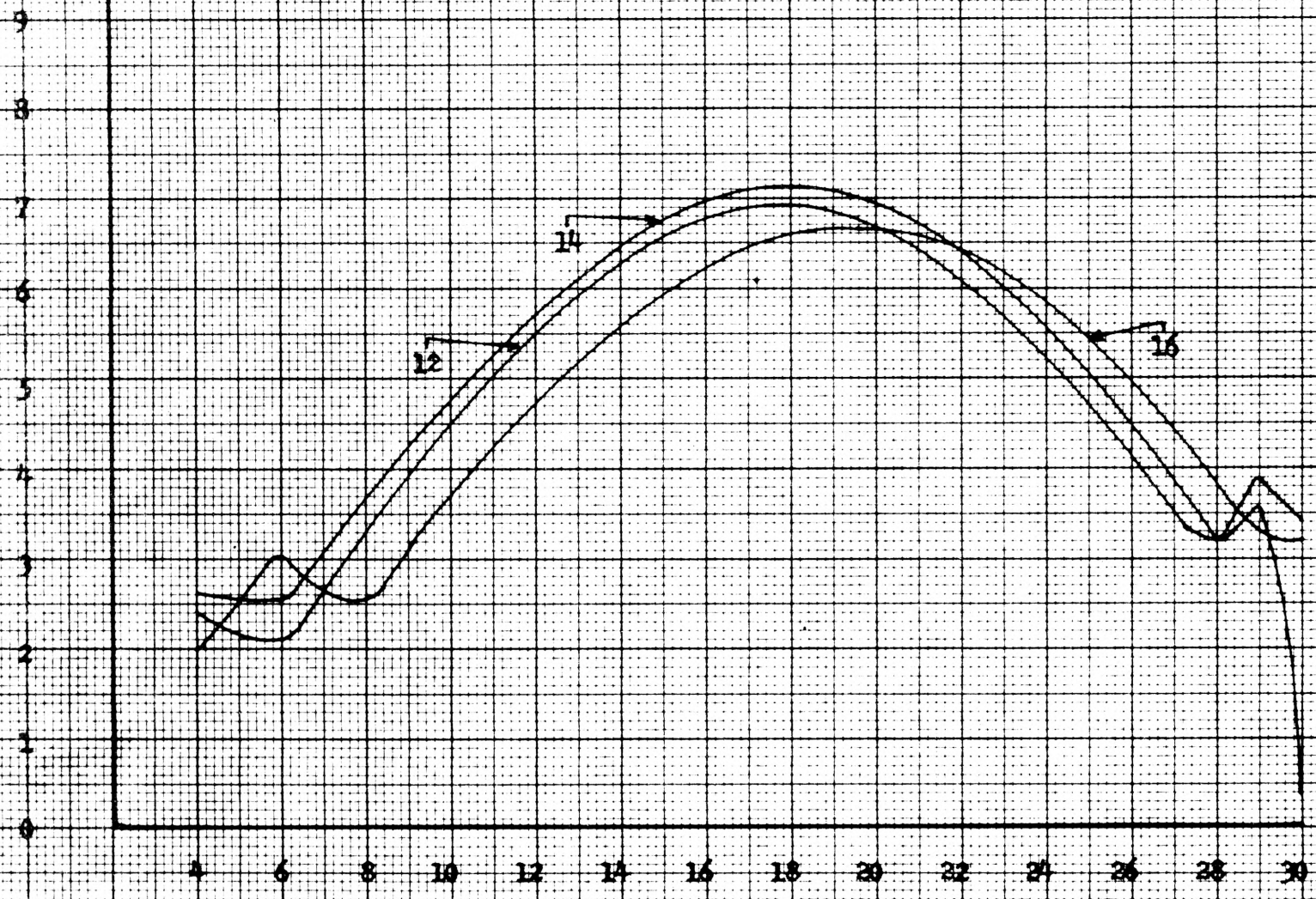


FIGURE 7a

FLUX DISTRIBUTION OF FUEL IN ROW C FOR 197

TABLE IV WIRE ACTIVATION FOR 19T

## General Information :

Irradiation date : May 22, 1962  
 Reactor power : 10 kilowatts  
 Critical time : 9:02 A.M.  
 Level time : 9:11:10 A.M.  
 Period of the reactor : 62 seconds  
 Scram time : 9:31:10 A.M.  
 Irradiation time : 20 minutes

## Wire No. 1

Position (inches)	N(counts per min.)	$t_2$ (decay <sup>2</sup> time)	$e^{-\lambda t_2}$	$\frac{N}{e^{-\lambda t_2}}$
30	1991	4 hr. 41 min.	.7774	2561
29	2680	" 42 "	.7767	3450
28	2085	" 43 "	.7761	2687
26	2762	" 44 "	.7754	3562
24	3430	" 45 "	.7747	4428
22	4025	" 46 "	.7740	5200
20	4381	" 48 "	.7726	5670
18	4226	" 49 "	.7719	5475
16	3993	" 51 "	.7706	5181
14	3863	" 52 "	.7699	5018
12	3465	" 53 "	.7692	4505
10	2739	" 54 "	.7685	3564
8	2035	" 55 "	.7678	2651
6	1473	" 56 "	.7672	1921
4	1709	" 57 "	.7665	2230
Average				4324



## Wire No. 2

Position (inches)	N(counts per min.)	$t_2$ (decay time)	$e^{-\lambda t_2}$	$\frac{N}{e^{-\lambda t_2}}$
30	393	22 hr. 21 min.	.3009	1306
29	1298	" 23 "	.3004	4322
28	1622	" 24 "	.3001	5404
26	2139	" 25 "	.2998	7136
24	2444	" 26 "	.2996	8157
22	2633	" 27 "	.2993	8796
20	2690	" 30 "	.2985	9012
18	2632	" 31 "	.2982	8826
16	2435	" 33 "	.2977	8179
14	2200	" 35 "	.2972	7402
12	1634	" 37 "	.2967	5507
10	1262	" 38 "	.2964	4258
8	1218	" 39 "	.2962	4112
6	874	" 40 "	.2959	2954
4	417	" 41 "	.2956	1411
Average				6869

## Wire No. 3

30	346	2 hr. 11 min.	.8893	388
29	4786	" 12 "	.8885	5386
28	5450	" 13 "	.8877	6139
26	6816	" 16 "	.8853	7699
24	7530	" 17 "	.8845	8513
22	8007	" 18 "	.8837	9061
20	8130	" 19 "	.8829	9209

## Wire No. 3

Position (inches)	N(counts per min.)	$t_2$ (decay <sup>2</sup> time)	$e^{-\lambda t_2}$	$\frac{N}{e^{-\lambda t_2}}$
18	7689	2 hr. 20 min.	.8821	8717
16	7358	" 21 "	.8813	8350
14	6585	" 23 "	.8796	7486
12	4509	" 24 "	.8788	5131
10	3741	" 25 "	.8780	4261
8	3703	" 26 "	.8772	4221
6	3078	" 27 "	.8764	3512
4	1595	" 28 "	.8756	1822
Average				7267

## Wire No. 4

30	248	21 hr. 56 min.	.3078	806
29	1271	" 57 "	.3075	4133
28	1229	" 59 "	.3070	4003
26	1726	22 hr.	.3067	5628
24	2107	" 1 min.	.3064	6877
22	2353	" 2 "	.3062	7685
20	2624	" 3 "	.3059	8578
18	2711	" 5 "	.3053	8880
16	2610	" 6 "	.3051	8555
14	2374	" 9 "	.3042	7804
12	2138	" 10 "	.3040	7033
10	1674	" 11 "	.3037	5512
8	1172	" 12 "	.3034	3863

## Wire No. 4

Position (inches)	N(counts per min.)	$t_2$ (decay <sup>2</sup> time)	$e^{-\lambda t_2}$	$\frac{N}{e^{-\lambda t_2}}$
6	1991	60 min.	9477	2101
4	2057	62 "	.9460	2173
Average.				3956

## Wire No. 5

30	59	0	1	
29	1842	1 min.	.9991	1843
28	1495	4 "	.9964	1500
26	2093	5 "	.9955	2102
24	2600	6 "	.9946	2613
22	3215	7 "	.9937	3235
20	3413	8 "	.9928	3438
18	3449	10 "	.9919	3480
16	3560	11 "	.9901	3596
14	3347	12 "	.9893	3383
12	3051	13 "	.9884	3087
10	2585	14 "	.9875	2617
8	2090	15 "	.9867	2118
6	1419	17 "	.9848	1440
4	1694	18 "	.9839	1721
Average				2834

## Wire No. 6

30	652	2 hr. 5 min.	.8941	729
29	1839	" 7 "	.8925	2060
28	1665	" 8 "	.8917	1667
26	2327	" 9 "	.8909	2612

## Wire No. 6

Position (inches)	N(counts per min.)	$t_2$ (decay time)	$e^{-\lambda t_2}$	$\frac{N}{e^{-\lambda t_2}}$
26	4379	5 hr. 21 min.	.7500	5839
24	5208	" 23 "	.7487	6956
22	5563	" 26 "	.7466	7451
20	5570	" 27 "	.7459	7467
18	5398	" 28 "	.7453	7243
16	5109	" 29 "	.7446	6861
14	4653	" 30 "	.7439	6255
12	3584	" 31 "	.7433	4822
10	2690	" 32 "	.7426	3622
8	2241	" 34 "	.7413	3023
6	1538	" 35 "	.7407	2076
4	706	" 36 "	.7387	954
Average				5584

## Wire No. 7

30	711	3 hr. 19 min.	.8367	850
29	5200	" 20 min.	.8359	6221
28	6013	" 21 "	.8352	7199
26	7633	" 22 "	.8344	9148
24	8266	" 24 "	.8329	9924
22	9346	" 25 "	.8321	11,232
20	9275	" 26 "	.8314	11,156
18	8931	" 27 "	.8306	10,752
16	8234	" 28 "	.8298	9923
14	6893	" 29 "	.8290	8315
12	5083	" 30 "	.8283	6137

## Wire No. 7

Position (inches)	N(counts per min.)	$t_2$ (decay <sup>2</sup> time)	$e^{-\lambda t_2}$	$\frac{N}{e^{-\lambda t_2}}$
10	3085	3 hr. 32 min.	.8268	3731
8	3145	" 33 "	.8260	3806
6	2348	" 37 "	.8232	2852
4	1150	" 38 "	.8225	1398
Average				7767

## Wire No. 8

30	2671	48 min.	.9579	2788
29	2978	49 "	.9570	3112
28	3436	50 "	.9562	3593
26	4541	52 "	.9545	4757
24	5174	53 "	.9536	5426
22	5884	54 "	.9528	6175
20	5987	55 "	.9519	6289
18	5898	56 "	.9511	6201
16	5876	58 "	.9494	6189
14	5142	59 "	.9485	5422
12	4267	1 hr. 00 "	.9477	4502
10	3301	" 01 "	.9469	3485
8	2287	" 02 "	.9460	2417
6	2698	" 03 "	.9452	2854
4	1601	" 06 "	.9426	1698
Average				4972

## Wire No. 9

Position (inches)	N(counts per min.)	$t_2$ (decay time)	$e^{-\lambda t_2}$	$\frac{N}{e^{-\lambda t_2}}$
30	2535	3 hr. 40 min.	.8211	3087
29	2733	" 41 "	.8202	3332
28	2065	" 42 "	.8195	2520
26	2925	" 43 "	.8188	3572
24	3693	" 45 "	.8173	4519
22	4431	" 46 "	.8167	5425
20	4773	" 47 "	.8160	5849
18	4975	" 48 "	.8153	6102
16	4964	" 50 "	.8138	6105
14	4714	" 51 "	.8131	5798
12	4099	" 52 "	.8124	5046
10	3193	" 53 "	.8117	3934
8	2463	" 55 "	.8102	3041
6	1527	" 56 "	.8095	1887
4	1716	" 57 "	.8088	2122
Average				4691

## Wire No. 10

30	4584	0 min.	1.0000	4584
29	5468	1 "	.9991	5472
28	5508	2 "	.9982	5518
26	7474	3 "	.9973	7494
24	8697	4 "	.9964	8728
22	9585	6 "	.9946	9637
20	10,299	7 "	.9937	10,364

## Wire No. 10

Position (inches)	N(counts per min.)	$t_2$ (decay <sup>2</sup> time)	$e^{-\lambda t_2}$	$\frac{N}{e^{-\lambda t_2}}$
18	10594	8 min.	.9928	10671
16	9312	9 "	.9919	9388
14	8938	11 "	.9893	9027
12	7682	12 "	.9893	7765
10	6273	13 "	.9884	6347
8	4368	14 "	.9875	4423
6	3629	15 "	.9867	3678
4	3104	18 "	.9839	3155
Average				8048

## Wire No. 11

30	1816	1 hr. 52 min.	.9046	2008
29	3207	" 53 "	.9038	3548
28	2432	" 54 "	.9030	2694
26	3175	" 55 "	.9022	3519
24	3879	" 56 "	.9014	4303
22	4453	" 58 "	.8998	4949
20	4850	" 59 "	.8990	5406
18	5253	2 hr.	.8981	5849
16	5062	" 1 min.	.8973	5641
14	4665	" 2 "	.8965	5204
12	4165	" 4 "	.8949	4654
10	3414	" 5 "	.8941	3819
8	2647	" 6 "	.8933	2964

## Wire No. 11

Position (inches)	N(counts per min.)	$t_2$ (decay <sup>2</sup> time)	$e^{-\lambda t_2}$	$\frac{N}{e^{-\lambda t_2}}$
6	1821	1 hr. 7 min.	.8925	2040
4	2117	" 9 "	.8909	2376
Average				4425

## Wire No. 12

30	2598	5 hr.	.7644	3399
29	2936	" 1 min.	.7637	3845
28	2406	" 2 "	.7630	3153
26	3127	" 3 "	.7624	4102
24	4071	" 5 "	.7610	5350
22	4629	" 6 "	.7603	6088
20	5034	" 7 "	.7596	6627
18	5177	" 8 "	.7589	6822
16	5211	" 9 "	.7582	6873
14	4605	" 10 "	.7576	6078
12	4142	" 12 "	.7562	5478
10	3293	" 13 "	.7555	4360
8	2325	" 14 "	.7548	3080
6	1565	" 15 "	.7541	2075
4	1805	" 17 "	.7528	2398
Average				5226

## Wire No. 14

30	293	2 hr. 49 min.	.8595	340
29	3046	" 50 "	.8587	3547



## Wire No. 14

Position (inches)	N(counts per min.)	$t_2$ (decay <sup>2</sup> time)	$e^{-\lambda t_2}$	$\frac{N}{e^{-\lambda t_2}}$
28	2750	2 hr. 51 min.	.8580	3205
26	3797	" 52 "	.8572	4430
24	4853	" 54 "	.8557	5671
22	5480	" 55 "	.8549	6410
20	5980	" 56 "	.8542	7001
18	6011	" 57 "	.8534	7043
16	5950	" 58 "	.8527	6978
14	5461	" 59 "	.8519	6411
12	5028	3 hr. 1 min.	.8504	5913
10	4122	" 2 min.	.8496	4852
8	3109	" 3 "	.8488	3663
6	2140	" 5 "	.8473	2526
4	2230	" 6 "	.8466	2635
Average				5569

## Wire No. 16

30	2935	1 hr. 11 min.	.9384	3128
29	3086	" 12 "	.9375	3292
28	3595	" 13 "	.9367	3838
26	4704	" 15 "	.9350	5031
24	5631	" 16 "	.9341	6028
22	6043	" 18 "	.9324	6481
20	6175	" 19 "	.9316	6628
18	5939	" 20 "	.9308	6381
16	5617	" 21 "	.9299	6041

## Wire No. 16

Position (inches)	N(counts per min.)	$t_2$ (decay <sup>2</sup> time)	$e^{-\lambda t_2}$	$\frac{N}{e^{-\lambda t_2}}$
14	5252	1 hr. 22 min.	.9291	5653
12	4466	" 23 "	.9282	4811
10	3437	" 25 "	.9265	3709
8	2301	" 26 "	.9257	2485
6	2821	" 27 "	.9248	3050
4	1787	" 28 "	.9239	1934
<b>Average</b>				5292

TABLE V GOLD FOIL ACTIVATION FOR 19T

## A. Bare Gold Foils

## General Information :

Irradiation date : May 25, 1962  
 Reactor power : 10 watts  
 Critical time : 9:30 A.M.  
 Level time : 9:34:30 A.M.  
 Period of the reactor : 48 seconds  
 Scram time : 9:44:30 A.M.  
 Irradiation time : 10 minutes

Core Position	Vertical Position (inches)	Foil Mass (grams)	N(counts per 15 min.)	$t_2$ (decay <sup>2</sup> time)	Saturation Counts
F-4	18	.1088	153,626	3 days 30 min.	$7.021 \times 10^{10}$
F-4	14	.1142	153,217	3 days 13 min.	$6.981 \times 10^{10}$
F-6	18	.1144	162,538	3 days 46 min.	$7.449 \times 10^{10}$
F-6	14	.1144	148,563	3 days 63 min.	$6.829 \times 10^{10}$

## B. Cadmium Covered Gold Foils

## General Information :

Irradiation date : May 25, 1962

Reactor power : 10 watts

Critical time : 10:09 A.M.

Level time : 10:12:40 A.M.

Period of the reactor : 57.5 seconds

Scram time : 10:22:40 A.M.

Irradiation time : 10 minutes

Core Position	Vertical Position (inches)	Foil Mass (grams)	N(counts per 15 min.)	$t_2$ (decay time)	Saturation Counts
F-4	18	.1088	25,495	5 hr. 5 min.	$5.664 \times 10^9$
F-4	14	.1142	30,558	4 hr. 54 min.	$6.776 \times 10^9$
F-6	18	.1144	27,151	3 hr. 57 min.	$5.959 \times 10^9$
F-6	14	.1144	25,946	4 hr. 24 min.	$5.722 \times 10^9$

## IV CONCLUSIONS

From the results of this investigation, the flux of the reactor at 10 kilowatt lies between  $7.24 \times 10^{10}$  and

$7.87 \times 10^{10} \frac{\text{neutrons}}{\text{cm}^2 \text{ sec}}$  for 19W arrangement, and for 19T, the

flux lies between  $10.71 \times 10^{10}$  and  $11.89 \times 10^{10} \frac{\text{neutrons}}{\text{cm}^2 \text{ sec}}$ .

This discrepancy of the average flux for the two core geometries is understandable since the power level calibration is true for only one arrangement. In the calculation for the average flux, the flux contribution of fuel elements at D-4, E-4, E-6, and D-6 were neglected. Due to the flux depressions by the control rods, the inclusion of the flux contribution from the above fuel elements would lower the average flux of the 19T arrangements. The effect of the 19T geometry to the compensated ionization chamber is uncertain. In this geometry the proximity of the chamber to the thermal column and wall apparently produced a net effect of smaller ionization current.

The appearance of the two water wings, grouped about 6 inches and 28 inches, shows the effect of water as the neutron reflector. The less pronounced wing is at 6 inches; this is due to the absorption of neutrons by the wire holder. It is apparent the fuel plates are approximately 22 inches long, the distance between the water wings. This is verified by the x-ray photographs of the fuel elements.

All the flux distributions closely approximate cosine curves. Noting this and the core symmetry, it is possible to map the flux distribution by locating 15 inch wires at strategic positions. The result is less accurate but the saving of labor and time may justify this approach.

It is found that the largest uncertainty is the positioning of the wires inside the fuel elements. Due to the difficulties in maneuverability and visibility, it is extremely difficult to place wires at the identical position in each fuel element. However, this problem is not a hindrance if average flux of the core is needed. To overcome the lengthy procedure of counting and data processing, a system of automatic counting which feeds the data into the computer is needed. The automatic counting set-up can be devised with the aid of gears, drums and timers. The scalar output and the wire position are fed into the computer simultaneously to determine the flux and its position in the core. This information can be graphically plotted by a recorder and the average power of the reactor can be acquired. A very sophisticated wire activation set-up is discussed by Kompanek and Tarnuzzer (20).

The pure copper wire activation is practicable for thermal neutron flux between  $10^8 \frac{\text{neutrons}}{\text{cm}^2 \text{ sec}}$  to  $10^{12} \frac{\text{neutrons}}{\text{cm}^2 \text{ sec}}$ .

For lower neutron flux, the radioactivity induced would give poor counting statistic for reasonable counting time.

For higher thermal neutron flux,  $10^{12} \frac{\text{neutrons}}{\text{cm}^2 \text{ sec}}$  to  $10^{15} \frac{\text{neutrons}}{\text{cm}^2 \text{ sec}}$ , a dilute alloy of copper, copper titanium could

be used. Titanium has a small cross section for thermal neutrons and a fast decay half life, 5.8 minutes, for the induced activity, titanium-51. Thus the achieved activity is low and exposure to personnel handling will not be excessive without the need for lengthy storage.

## APPENDIX 1 SOLUTION OF THE NEUTRON ACTIVATION EQUATION

$$\frac{dN}{dt} = \sigma_a N_d S_d \phi - \lambda N$$

- $N$  : number of radioactive atoms at time  $t$   
 $\sigma_a$  : activation cross section of the detector for thermal neutrons  
 $N_d$  : molecular surface density of the detector  
 $S_d$  : surface area of the detector  
 $\phi$  : neutron flux of the reactor  
 $\lambda$  : decay constant of the detector

$$\text{let } k = \sigma_a N_d S_d \phi$$

$$\frac{dN}{k - \lambda N} = dt$$

$$- \frac{\ln(k - \lambda N)}{\lambda} = t + c$$

$$-\ln(k - \lambda N) = \lambda t + c'$$

$$k - \lambda N = e^{-\lambda t} e^{c'} = A e^{-\lambda t}$$

$$\text{when } t = 0, \quad N = 0$$

$$\text{thus } A = k \quad \text{and } N = \frac{k}{\lambda} (1 - e^{-\lambda t})$$

According to the decay law:

$$N_{t_2} = N e^{-\lambda t_2} \quad \text{and} \quad N_{t_2 + T} = N e^{-\lambda t_2} e^{-\lambda T}$$

- $N_{t_2}$  : number of radioactive atoms present at time  $t_2$   
 $N_{t_2+T}$  : number of radioactive atoms present at time  $t_2+T$   
 $t_2$  : time elapsed after the detector is removed from the flux

$$N_T = N_{t_2} - N_{t_2+T} = \frac{\sigma_a N_d S_d \phi}{\lambda} (1 - e^{-\lambda t_1}) (1 - e^{-\lambda T}) e^{-\lambda t_2}$$

$N_T$  : number of radioactive atoms decayed between  $t_2$  and  $t_2+T$

$t_1$  : time of irradiation



## APPENDIX 2 RADIOACTIVITY CORRECTION FOR REACTOR START-UP

## A. Solution of the Radioactivity Correction Equation for Reactor Start-Up

$$\frac{dN'}{dt} = \sigma_a N_d S_d \phi_0 e^{\frac{t}{T}} - \lambda N'$$

- $N'$  : contribution of radioactive atoms by reactor start-up
- $\sigma_a$  : activation cross section of the detector for thermal neutrons
- $N_d$  : molecular surface density of the detector
- $S_d$  : surface area of the detector
- $\phi_0$  : flux when the reactor is critical
- $t$  : time when the reactor is between critical and final power
- $T$  : period of the reactor while approaching final power
- $\lambda$  : decay constant of the detector

$$\text{let } k' = \sigma_a N_d S_d \phi_0$$

$$\frac{dN'}{dt} + \lambda N' = k' e^{\frac{t}{T}}$$

$$\frac{dN'}{dt} + \lambda N' = 0$$

$$N'_c = N'_0 e^{-\lambda t} \quad \text{complimentary solution}$$

$$N'_p = A e^{\frac{t}{T}} \quad \text{particular solution}$$

$$\left(\frac{d}{dt} + \lambda\right) A e^{\frac{t}{T}} = k' e^{\frac{t}{T}}$$

$$A \left(\frac{1}{T} + \lambda\right) = k' \quad \text{or} \quad A = \frac{k'}{\frac{1}{T} + \lambda}$$

$$N' = N'_c + N'_p = N'_0 e^{-\lambda t} + \frac{k'}{\frac{1}{T} + \lambda} e^{\frac{t}{T}}$$

when  $t = 0$ ,  $N' = 0$

$$\text{thus } N'_0 = \frac{-k'}{\frac{1}{T} + \lambda}$$

$$N' = \frac{k'}{\frac{1}{T} + \lambda} (e^{\frac{t}{T}} - e^{-\lambda t})$$

$$N'_T = \frac{\sigma_a N_d S_d \phi_0}{\frac{1}{T} + \lambda} (e^{\frac{t}{T}} - e^{-\lambda t}) (1 - e^{-\lambda t}) e^{-\lambda t_2}$$

$N'_T$ : number of radioactive atoms contributed by the reactor start-up in the interval  $T$  after a decay time  $t_2$

#### B. Percentage Contribution of Radioactivity due to the Reactor Start-Up

For 19W wire run:

$t$  (time between critical and final power): 11 minutes

$T$  (period of the reactor while approaching critical)  
70 seconds

$\phi_0$  (flux when the reactor is critical at  $\frac{1}{10}$  watt)  
 $\propto \phi(10 \text{ kw}) \times 10^{-5}$

$\frac{N'_T}{N_T}$ : percentage of radioactive contribution due to the reactor start-up

$$\frac{N'_T}{N_T} = \frac{\frac{\sigma_a N_d S_d \phi(10 \text{ kw})}{\frac{1}{T} + \lambda} 10^{-5} (e^{\frac{t}{T}} - e^{-\lambda T}) (1 - e^{-\lambda T}) e^{-\lambda t_2}}{\frac{\sigma_a N_d S_d \phi(10 \text{ kw})}{\lambda} (1 - e^{-\lambda t_1}) (1 - e^{-\lambda T}) e^{-\lambda t_2}}$$

$$\frac{N_T^i}{N_T} = \frac{10^{-5} (e^{\frac{t}{T}} - e^{-\lambda t})}{(\frac{1}{T} + \lambda) (1 - e^{-\lambda t_1})}$$

$$\frac{N_T^i}{N_T} = \frac{1.492 \times 10^{-5} \times 10^{-5} \times 1.23 \times 10^4}{1.43 \times 10^{-1} \times 1.79 \times 10^{-2}} = 0.07 \%$$

## APPENDIX 3 SAMPLE COMPUTATIONS

## A. Standard Foil Computation

standard gold foil: 1/2 inch diameter, 0.002 inch thick, and  $m_s$  (mass) 0.1168 gram

$\phi_s$  (standard flux of National Bureau of Standards):

$$4.23 \times 10^3 \frac{\text{neutrons}}{\text{cm}^2 \text{- sec}}$$

time in: May 7, 1962 at 9:55 A.M. EST

time out: May 14, 1962 at 2:15 P.M. EST

$t_1$  (total time of irradiation): 7 days, 4 hours and 20 minutes

$T$  (total counting time): 50 minutes

$t_2$  (total decay time): 2 days, 18 hours, and 21 minutes

half life of gold activity: 2.7 days

decay constant,  $\lambda$ , :  $\frac{0.693}{2.7} \text{ days}^{-1}$

$N$  (total number of counts less background): 6599

$N_s$  (saturation number of counts for 100% counting geometry and 100% counter efficiency):

$$N_s = \frac{6599}{(1 - e^{-\lambda t_1}) (1 - e^{-\lambda T}) e^{-\lambda t_2}} = 1.7972 \times 10^6$$

## B. Absolute Flux Calculation of Core Position F-6 at 18 Inches

Since  $N_s \propto m_s \phi_s$ , it follows that the saturation counts registered in the same scalar and counting geometry for any gold foil of similar physical dimension is also proportional to the mass and flux.

$$\phi' = \phi_s \frac{N'_s m_s}{N_s m'} = 4.23 \times 10^3 \frac{N'_s 0.1168}{1.7972 \times 10^6 m'}$$

$N'$  (saturation counts of bare gold foil) :  $5.7083 \times 10^{10}$

$m'$  (mass): 0.1085 gram in the reactor operating at 10 watts

$t_1$  (irradiation time) : 10 minutes

$T$  (counting time) : 15 minutes

$t_2$  (decay time) : 3 days and 33 minutes

$N'_s$  (saturation counts of cadmium covered gold foil) :  
 $1.7866 \times 10^{10}$

$t_1$  (irradiation time in the reactor operating at 10 watts) : 10 minutes

$T$  (counting) : 15 minutes

$t_2$  (decay time) : 1 hour and 53 minutes

$N'_s$  (saturation counts due to thermal neutrons) =

$$5.7083 \times 10^{10} - 1.7866 \times 10^{10} = 3.9217 \times 10^{10}$$

$$\phi' (10 \text{ watts}) = 4.23 \times 10^3 \frac{3.9217 \times 10^{10} \cdot 0.1168}{1.7972 \times 10^6 \cdot 0.1085}$$

$$= 9.94 \times 10^7 \text{ neutrons/cm}^2\text{-sec}$$

C. Average Absolute Flux Calculation of the core

For the identical position, the saturation counts of the wire irradiation experiment for the reactor at 10 kilowatts is 4991.

thus  $4991 \text{ counts} \propto 9.945 \times 10^{10} \text{ neutrons/cm}^2\text{-sec}$

$\bar{\phi}(10 \text{ kw})$  (average thermal flux of the reactor at 10 kilowatts and 19W geometry) =  $9.945 \times 10^{10} \frac{3645}{4991} = 7.24 \times 10^{10} \text{ neutrons/cm}^2\text{-sec}$

3645 is the average saturation counts of the reactor at 19W.

## BIBLIOGRAPHY

1. Janowski, F. and A. Wattenberg (1950) A Method for the Determination of Neutron Flux. AECD-3082.
2. Greenfield, M. A., Koontz, Jarrett, and Taylor (1957) Measuring Flux Absolutely with Indium Foil. Nucleonics 15, No. 3, p. 57.
3. Vignon, M. A. and L. Diez (1956) Perturbation of Neutron Densities by Foils. Anales real soc. espan fis y quim (Madrid) Serial A. 52A, p.5.
4. Martin, H. D. (1954) Correction Factors for Measurements with Cadmium. NAA-SR-1076.
5. Klickman, Cunningham, Chastain, Keller, and Fawcett (1956) A Wire-Activation Technique for Reactor-Flux-Profile Measurements. BMI-1086.
6. Fowler, I. L. and P. R. Tunncliffe (1950) Boron Trifluoride Proportional Counters. Rev. Sci. Instr. 21, p. 734.
7. Hansen, A. O. and J. L. McKibben (1947) A Neutron Detector Having Uniform Sensitivity from 10 kev to 3 mev. Phys. Rev. 72, p. 673.
8. Wiegand, C. (1948) High Energy Neutron Detector. Rev. Sci. Instr. 19, p. 790.
9. Rossi, B. B. and H. H. Staub (1949) Ionization Chambers and Counters. McGraw-Hill. New York chapter 9.
10. Baer, W. and R. T. Bayard (1953) A High Sensitivity Fission Counter. Rev. Sci. Instr. 24, p. 138.
11. Allen, W. D. and A. T. G. Ferguson (1955) A Fission Counter with Fissile Material Density for Fast Neutron Fission Counting. J. Nuclear Energy 2, p. 38.
12. Nobles, R. G. and A. B. Smith (1956) Fission Chamber Measures Neutron Distribution Quickly, Accurately. Nucleonics 14, No. 1, p. 60.
13. Cohen, B. L. (1951) High-Energy Neutron Threshold Detectors. Nucleonic 8, No. 2, p. 29.
14. Hurst, G. S., et al. (1956) Techniques of Measuring Neutron Spectra with Threshold Detectors-Tissue Does Determination. Rev. Sci. Instr. 27, p. 153

15. Bolinger, L. M. (1956) Proceedings of the International Conference on the Peaceful Uses of Atomic Energy. 4, p.47.
16. McCrary, Taylor and Bonner (1954) A Fast Neutron Counter with Energy Resolution. Phys. Rev. 94, p. 808.
17. Rosen, L. (1953) Nuclear Emulsion Techniques for the Measurement of Neutron Energy Spectra. Nucleonics 11, No. 7, p. 32 and No. 8, p. 38.
18. Richard, H. T., et al. (1951) Proton Range-Energy Relation for Eastman NTA Emulsions. Phys. Rev. 83, p. 994.
19. Kompanek, Jr. A. J. and E. C. Tarnuzzer (1962) Neutron-Activated Wires Plot Fluxes in Yankee Core. Nucleonic 20, No. 2, p. 44.

## VITA

Cary, Chow-yuen, Chen was born on January 16, 1937 in Kwantung Province, China, the son of Kuak-Kiung and Shien Uion Chen. He attended elementary schools in China, Hong Kong, and Chicago, Illinois. He received his high school education from Norwalk High School, Norwalk, Connecticut, and graduated from it in 1955.

From 1955 to 1959, he attended Rensselaer Polytechnic Institute in Troy, New York and graduated in June, 1959, with the degree of B. S. in physics. In 1959 and 1960, he was employed as an electrical engineer at Sorensen and Co., Norwalk, Connecticut.

In September of 1960, he enrolled as a masters degree candidate in physics at Missouri School of Mines and Metallurgy, Rolla, Missouri. He was a teaching assistant in physics from September, 1961 to June, 1962.

He is a member of Sigma Pi Sigma.

